MULTIPHASE MODELING OF EROSION WEAR IN SLURRY PIPE

A Dissertation submitted
in partial fulfilment of the requirements
for the award of degree of

Master of Engineering

in

Thermal Engineering

by

Vikas Kannojiya

Registration No.: 801483025

Under the Supervision of

DR. SATISH KUMAR

(Assistant Professor)

DEPARTMENT OF MECHANICAL ENGINEERING

THAPAR UNIVERSITY, PATIALA

July, 2016

CERTIFICATE

I hereby declare that the thesis entitled "**Multiphase Modeling of Erosion Wear in Slurry Pipe**" is an authentic record of my work carried out as requirements for the award of the degree of **Master of Engineering** in **Thermal Engineering** at **Thapar University, Patiala** under the supervision of **Dr. Satish Kumar**, Assistant Professor, Mechanical Department, Thapar University, Patiala during July, 2014 to July, 2016. No part of the matter embodied in this report has been submitted to any other university or institute for the award of any degree.

Date: 05/07/2016

Vikas Kannojiya

It is certified that the above statement made by the student is correct to the best of my/our knowledge and belief.

Dr. Satish Kumar
Assistant Professor, MED
Thapar University, Patiala

Countersigned by

Dr. S.K. Mohapatra
Head, Mechanical Engineering Department
Thapar University, Patiala-147004

Dr. S.S. Bhatia
Dean of Academic Affairs
Thapar University, Patiala-147004

Dedication

I dedicate this thesis to my beloved father Late Manoj Kannojiya and my mother Kanchan Kannojiya, who are an ever supporting and encouraging with their great patience. I also dedicate this to my brother Vishal Kannojiya, who stood as an impression and to all my dearest friends.

ACKNOWLEDGEMENTS

First of all, I would like to thanks to my most esteemed supervisors Dr. Satish Kumar and for their worthy guidance, continuous encouragement and having high patience to listen to all my queries and suggest accordingly. The faith of Dr. Satish Kumar in me always compelled me to work hard, apart from thesis his attitude towards life, work and valuable words taught me many things.

I appreciate the facilities provided by Thapar University to carry out my studies and gain practical knowledge. I gratefully acknowledge SAI labs, Thapar University for providing the results in time.

A special debt of gratitude is owed to the authors whose work I have consulted and quoted in this work.

Last but not least I am always grateful to my family and friends for their unconditional support, encouragement and best wishes, without which I have not come this far.

Vikas Kannojiya

Abstract

Erosion wear is a serious problem faced in many industries like chemical industries, gas extraction, mining, power generation. In Indian thermal power plants, approximately 30% of ash is produced as a side product while generating power. This ash possesses highly abrasive characteristics. Pipe line is believed to be economical and eco-friendly way of slurry transport rather than the rail transport or road transport. Due to the presence of abrasives in slurry, a problem of wear is often observed in the pipe lines while conveying it to the ash well for the disposal purpose. Erosion causes the degradation or removal of pipe line material which may results in the failure of pipe. Prevention of piping and tubing from getting eroded is therefore an essential objective. Erosion wear gets influenced by different operating parameters like flow velocity, particle attributes, target property, impact angle etc and thus a complicated phenomenon to understand. Several researches were going on to analyse the influence of different operating parameters on the erosion wear.

In this work, computational technique is used to analyse erosion wear of mild steel pipe bend caused by the bottom ash-water slurry. Computational Fluid Dynamics (CFD) code FLUENT 15.0 is applied to investigate the influence of pipe diameter, bending angle, flow velocity and bending radius ratio. Simulation study is carried by considering several pipe bends of different diameters from 50 to 200 mm, bending angles in range of 45 to 90^0 and bending radius of 1.5 to 2.5 at flow velocity variation from 2 to 8 m/s An Euler-Lagrange model with Standard k-ϵ modelling scheme along with the mixture property was implemented in this work to solve the multiphase flow through the pipe line. The magnitude and location of erosion wear is reported at different operating conditions. The obtained results show good agreement with the previous published findings of several investigators.

Key words: Multiphase flow, Pipe erosion, Slurry transport, CFD, FLUENT

TABLE OF CONTENTS

LIST OF FIGURES

LIST OF TABLES

LIST OF SYMBOLS AND ABBREVIATIONS

Nomenclature

A	Cross section area of pipe (m^2)
D	Pipe diameter (m)
F_b	Buoyancy force (N)
F_d	Fluid drag force (N)
F_g	Gravitational force (N)
g	Acceleration due to gravity (ms^{-2})
d_p	Particle Diameter (m)
m_p	Particle mass
n	Exponent
P	Pressure (Pa)
T	Time (s)
Re	Reynolds number
K	Turbulence kinetic energy (m^2s^{-2})
V_f	Particle Relative velocity (ms^{-1})
U_P	Particle Velocity (ms^{-1})

Greek symbols

μ_{eff}	Effective viscosity for fluid phase (Pa.s)
ρ_f	Fluid Density (kgm^{-3})
ρ_p	Particle density (kgm^{-3})
ρ_b	Bulk density (kgm^{-3})
Φ	Particle volume Fraction

Acronym

ESP	Electro Static Precipitator
CFD	Computational Fluid Dynamics
DPM	Discrete Phase Modeling
DEM	Discrete Element Method

CHAPTER 1

INTRODUCTION

The world power transportation system comprises of more than million miles of pipelines. Pipelines assumed to be an essential part in our day by day lives. Cooking and cleaning, the day by day drive, air travel and the warming of homes and organizations are all made conceivable by the fuel conveyed through pipelines. Many components of the pipe used in power generation, gas extraction, chemical industries etc are subjected to the erosion problem causes significant loss of material or production.

In Indian thermal power generation plants, approximately 207 Metric tonnes of ash (fly ash + bottom ash) is produced from 594 Metric tonnes of feeded coal for the generation of 96.74 giga watts, this ash possesses highly abrasive characteristics. Out of this total ash an approximate 20% share is of bottom ash[1]. Pipe line is believed to be economical and eco-friendly way of slurry transport rather than the rail transport or road transport. The disposal of ash (Fly ash + Bottom ash) generated in a thermal power plant during the power production process is always a concern which have to be solved. Due to the presence of abrasives in slurry, a problem of wear is often observed in the pipe lines while conveying it to the ash well for the disposal purpose[2]. Many components of the machinery used in power generation, gas extraction, chemical industries etc are subjected to the erosion problem causes significant loss of material or production.

If the erosion wear is not properly located, predicted and controlled then the entire process will be suffered and there can be even pipe failure, production losses and safety issues. The estimation of erosion caused by the multiphase flow of solid and liquid is a very complicated issue due to the involvement of several affecting parameters (eg. Flow velocity, particle concentration, particle size, attributes of target material). Several research/investigations were conducted to analyse the influence of parameters on the erosion rate.

1.1 Thermal Power Plant Ash Disposal System

The coal fired thermal power plant generates large quantity of ash, besides the energy generation. Out of the total generated ash, there is approximately 20% of bottom ash and 80% of fly ash.

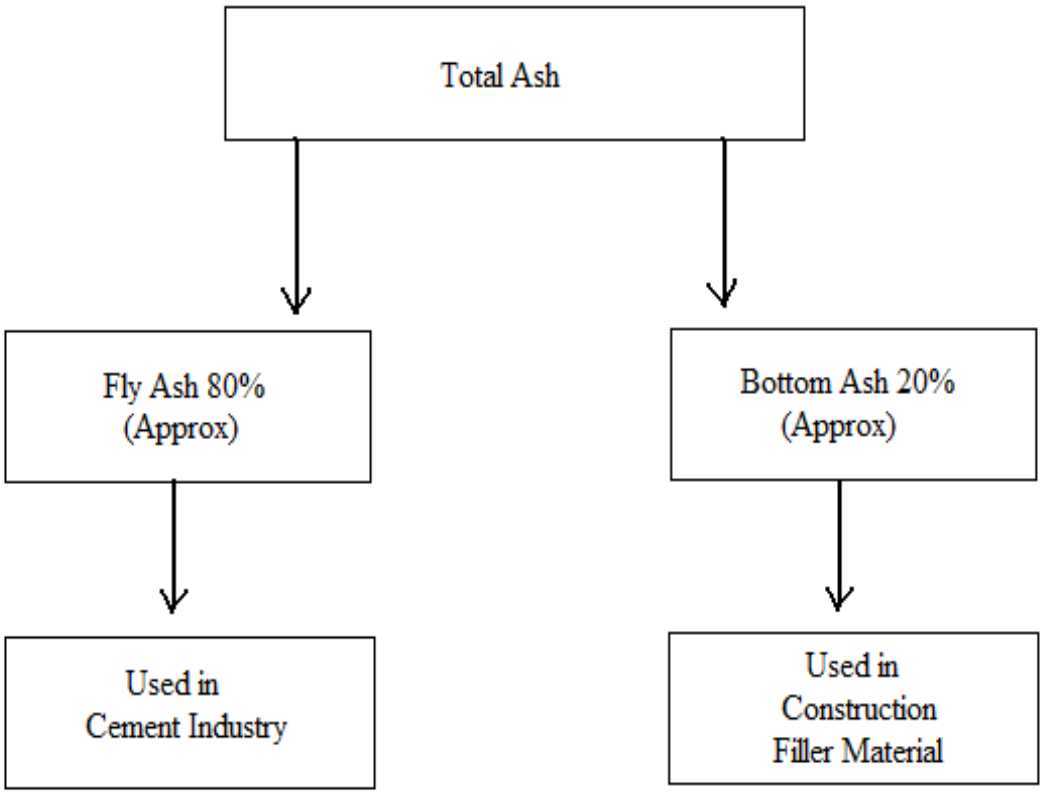

Figure 1.1: Ash distribution

The fine ash particles which rise along the flue gases are known as fly ash. The fly ash is collected through electrostatic precipitator and is sent to the utilization unit by passing it through the fly ash handling unit. While the clinkers formed by the residue of un-burnable material are known as bottom ash. The clinkers are crushed into smaller size, mixed with water to form slurry and then conveyed to the utilization unit through bottom ash handling unit. A typical layout of ash distribution of a thermal power plant is shown in Figure1.2.

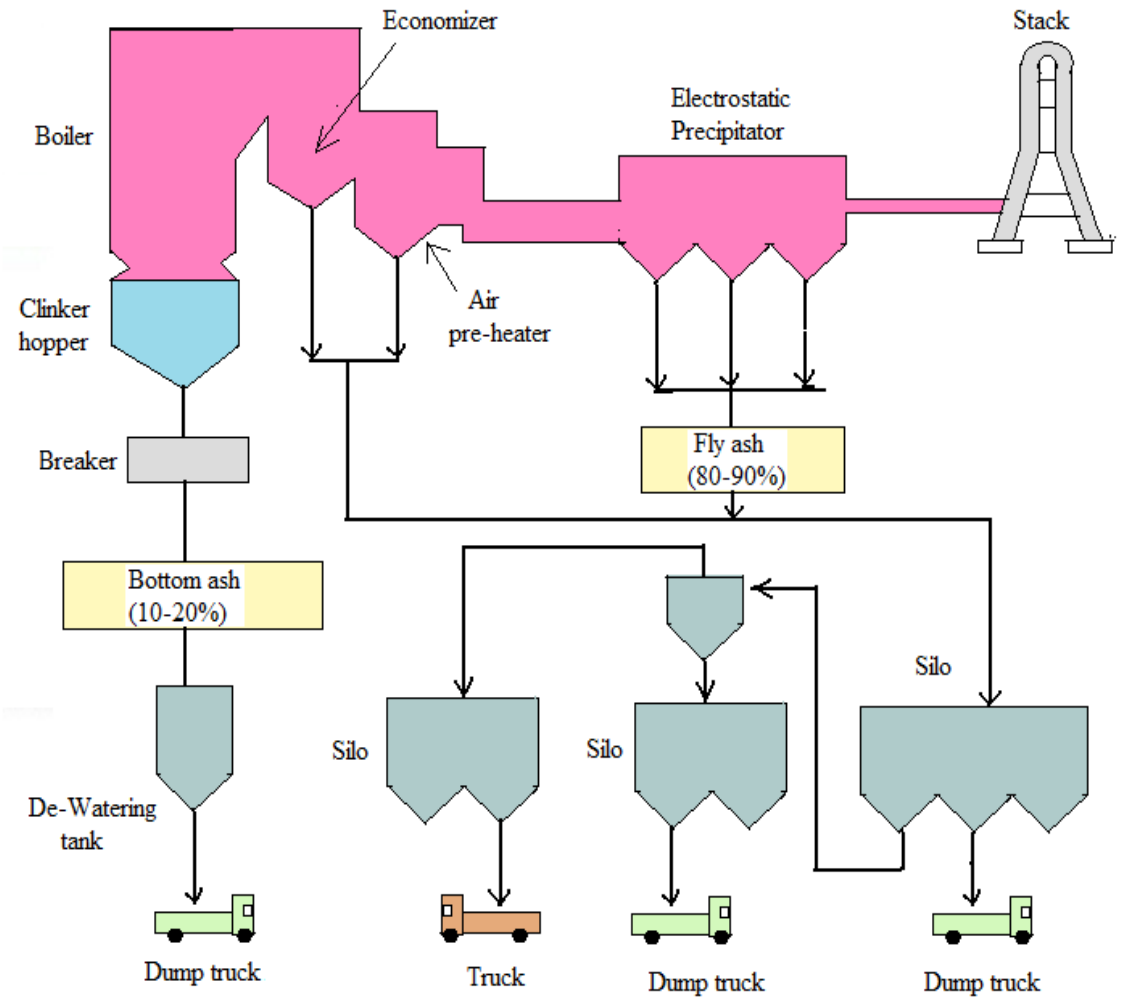

Figure 1.2: Schematic of ash distribution in a power plant

1.2 Ash Handling System

In a thermal power plant, the generated ash can be categorized as fly ash and bottom ash. There is different mechanism for handling these different type of ashes. Fly ash is finer in size and can be transported through pneumatic conveying. While being heavier and larger in size, bottom ash is transported through hydraulic conveying in the form of slurry comprising water content in it.

Ash handling systems can be divided into two categories-

a) Dry ash handling unit

b) Wet ash handling unit

1.2.1 Dry (Fly) Ash Handling System

The finer un-burnt residue of coal combustion which is carried along with the flue gases are fly ash. The generation of fly ash occurs in a huge amount in any thermal plant and it contributes about 80% of total ash. In the ancient time fly ash was used to be disposed directly to the atmosphere. But due to its polluting affects, various researches have been conducted to obtain a proper disposal system of fly ash. Figure 1.3 shows the layout of fly ash disposal system.

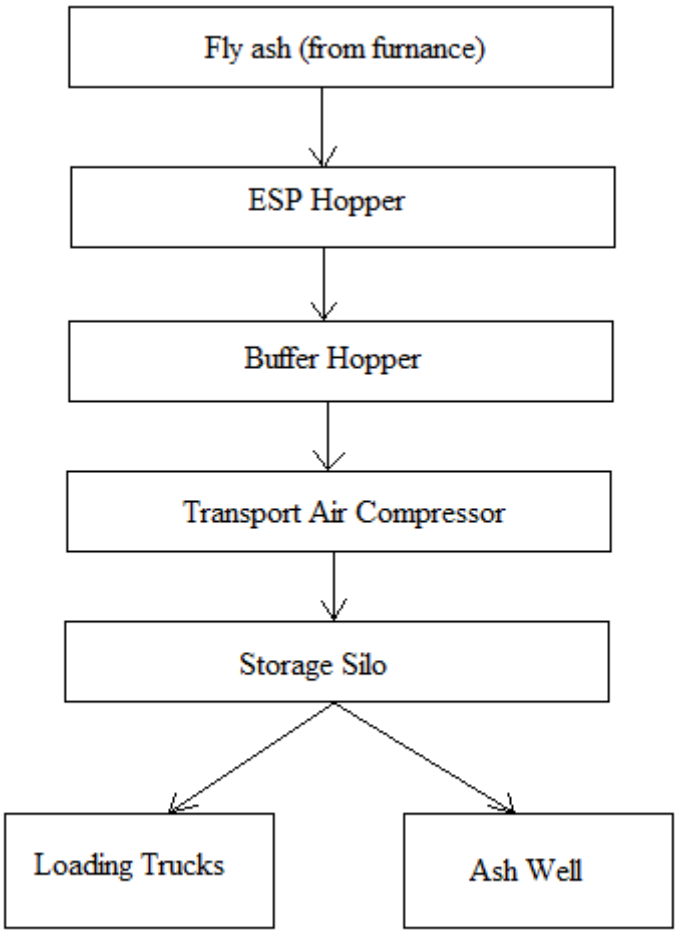

Figure 1.3: Components of fly ash handling unit

Fly ash is carried along with the flue gases and is passed though economiser, air-preheater and is finally captured when it passes through the electro-static precipitator. The captured fly ash is stored in ash hoppers, from where it is conveyed by a air compressor to the silo and then to the utilization unit.

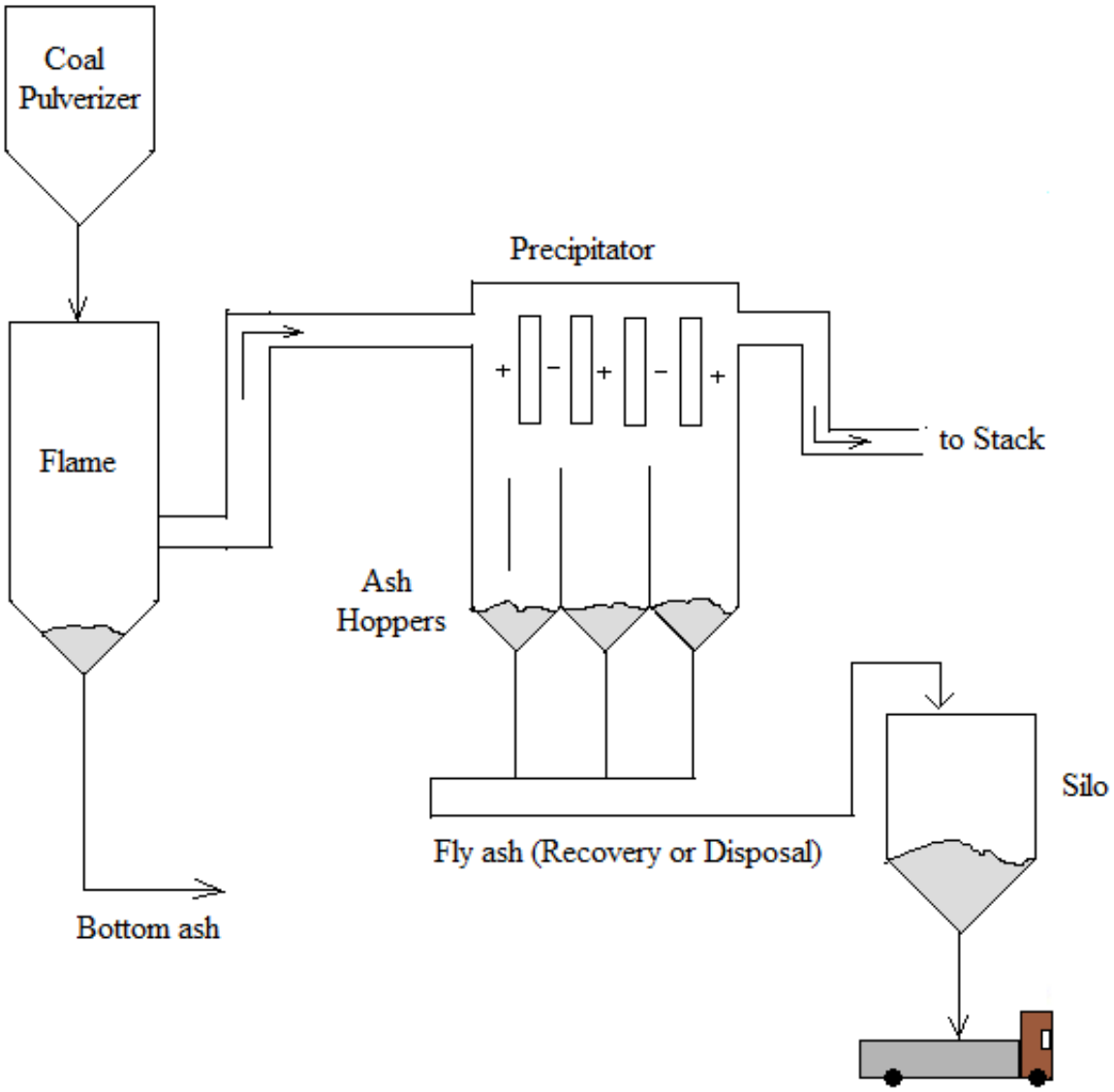

Figure 1.4: Fly ash conveyance layout

1.2.2 Wet Ash (Bottom Ash) Handling System

The clinker formation due to the un-burnt residue of coal in a thermal plant is the bottom ash. The generation of bottom ash in a power plant is up to 10-20% of the total ash content[3]. Figure 1.5 shows the basic component of a wet ash handling unit.

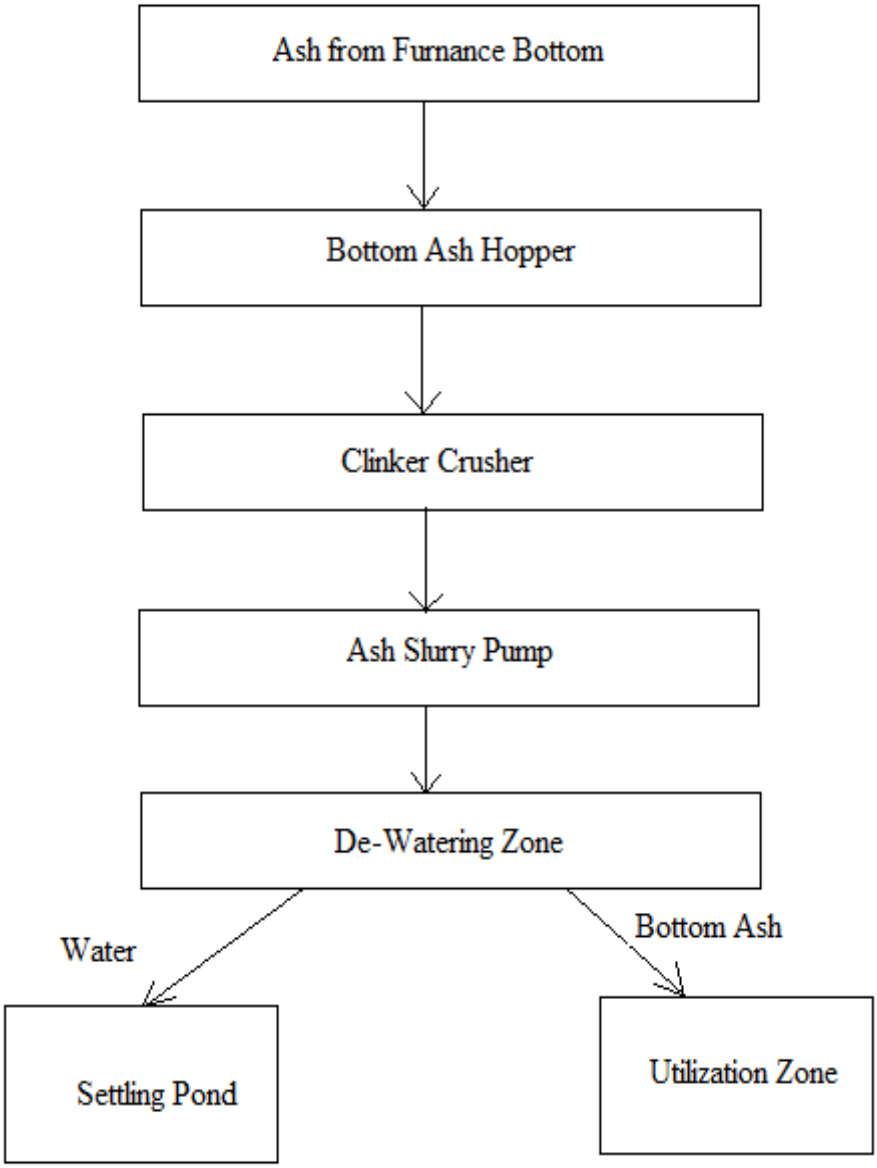

Figure 1.5: Components of bottom ash handling system

The bottom ash is mixed with water to form slurry and is conveyed to Dewatering zone. From the Dewatering zone the water is extracted from the slurry and is sent to the storage silos from where it can be utilised as a road construction material, foundation filling material etc. A generalised lay out of the bottom ash conveying system is shown in figure 1.6.

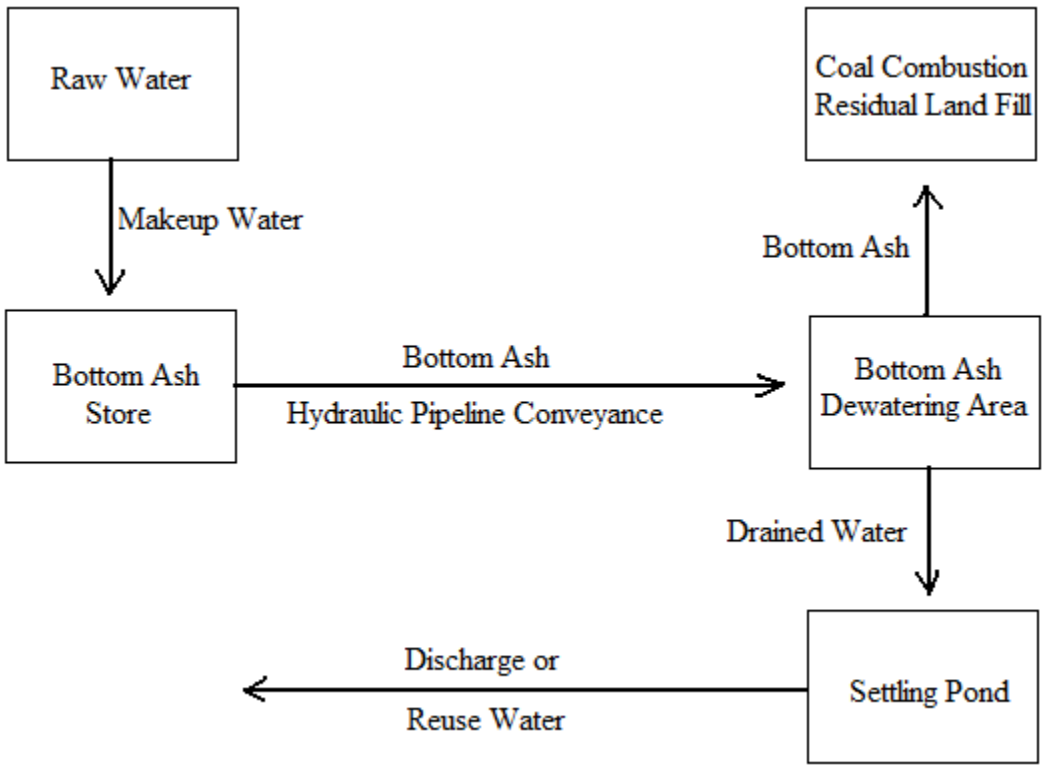

Figure 1.6: Bottom ash conveyance layout

1.3 Slurry Transport System

Energy generation in thermal power plants by burning the feed coal generates a large amount of ash as a side product. The most common method to transport this coal ash to the disposal unit is by using slurry pipe line. Ash is transported through the pipe line in the form of slurry, from the slurry preparation unit to the utilization zone. Ash is crushed into smaller and uniform size by crusher in the slurry preparation unit and is stored in the storage unit. From the storage unit it is pumped to the utilization zone after passing through the dewatering zone. Figure 1.7 shows the basic component and procedure of slurry transport

The primary component of a slurry transport unit as listed below-

a) Slurry preparation unit

b) Pipe lines

c) Slurry pumps

d) Dewatering unit

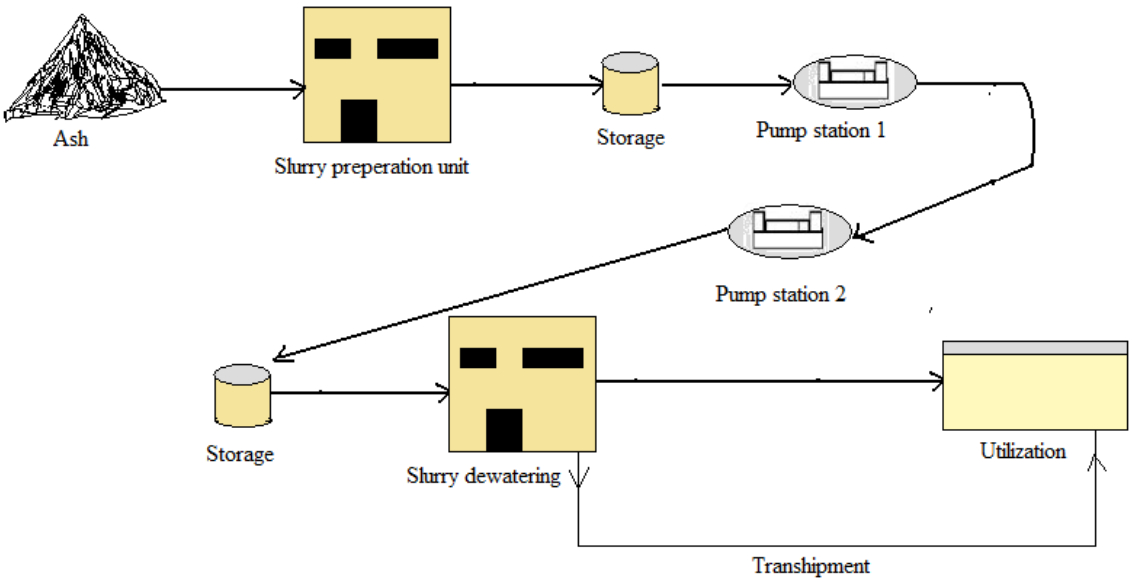

Figure 1.7: Basic component of slurry transport system

1.4 Wear

Wear is the process of material removal from either of the two mating surface having rolling or sliding motion with respect to each other. Wear is responsible to reduce the durability and response characteristics of almost all of the machines. Therefore, a thorough investigation and deep preventive measures are to be taken to reduce the wear problems associated with the industrial components. The wear occurrence depends on load applied, sliding and rolling velocities, mechanical properties, geometry of the surfaces etc.

1.5 Types of wear

Wear can be broadly categorised as

Adhesive wear

Abrasive wear

Fatigue wear

Corrosive wear

Erosion wear

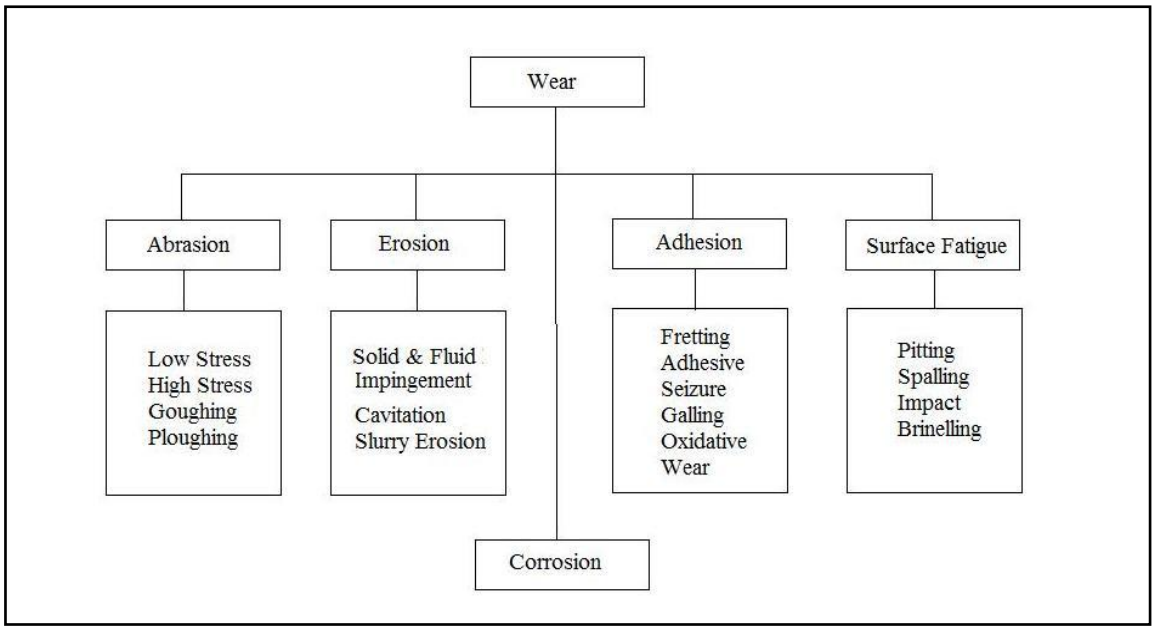

Figure 1.8: Classification of Wear

Adhesive wear

This is also known as frictional wear. Such wear is found when the two surfaces are in frictional contact with each other. An unwanted removal of material due to plastic deformation takes places when the two surfaces having relative motion with each other with a direct contact.

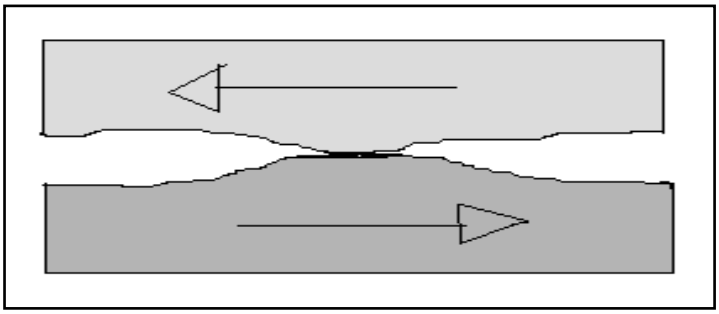

Figure 1.9: Adhesive wear

Abrasive wear

When a hard material with rough surface slides across a comparatively softer material surface then a material removal is observed from the softer material such a wear is called as Abrasive wear. It can be said as the loss/removal of material/substance due to comparatively hard particles that are sliding over the softer material.

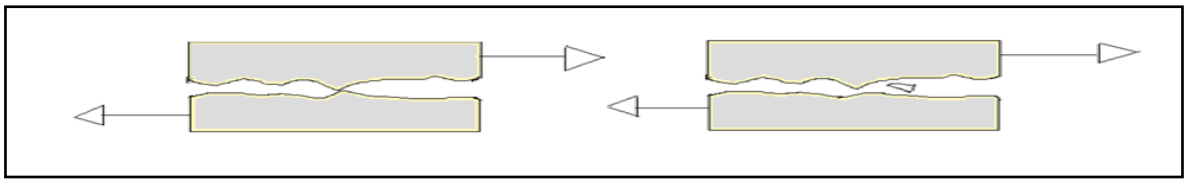

Figure 1.10: Abrasive wear

Fatigue wear

The removal of material occurs when the two surfaces are in pure rolling contact or rolling with sliding contact with each other. It is mainly found in bearings, to avoid this wear the surfaces of most of the bearings are surface hardened.

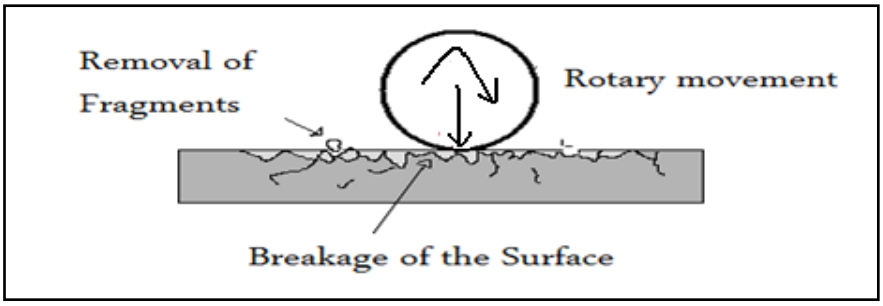

Figure 1.11: Fatigue wear

Corrosive wear

In corrosive wear, due to some environmental conditions a reaction product is formed in either one or both of the contact surfaces. This product is then removed due to the rubbing action of the surfaces.

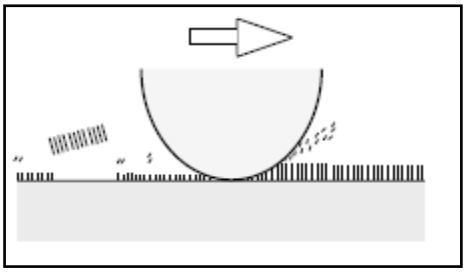

Figure 1.12: Corrosive wear

Erosive wear

The removal of matter from a surface triggered by the impingement of solid or droplets of liquid or gas against an object's surface then such type of wear are called as erosive wear.

The material is removed due to repeated impact of the particles. The pipe lines and tubing of industry are most the suffered components through this problem.

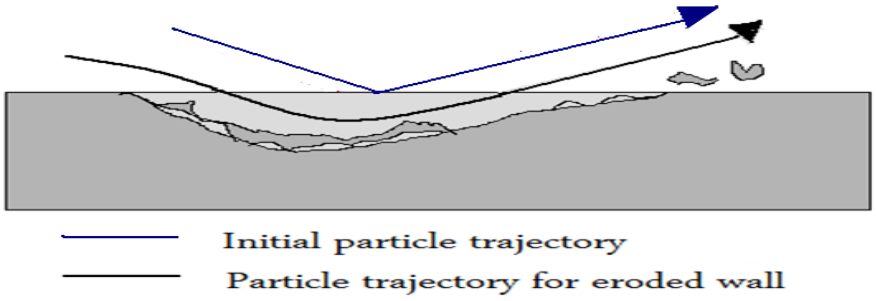

Figure 1.13: Erosive wear

1.6 Particulate Erosion Mechanism

A Proper relationship must be developed between the erosion wear of the material and the process parameters such as flow velocity, particle size, particle concentration and attribute of the target material in order to develop the equations predicting the erosion rate of mass removal of the material due to impact of particles. Particulate erosion mechanism can be divided into two category viz ductile erosive wear mechanism and brittle erosive wear mechanism. In brittle erosion mechanism the removal of material takes place due to cracking and chip formation. While in ductile erosion mechanism the removal of material takes place due to the ploughing and cutting mechanism

- **Mechanism for Ductile Material**

There are four different mechanism of erosion wear recognized for ductile material. Which are as follows:

Indenting Includes a distinctive attribute of surface indentation caused by plastic deformation.

Ploughing This mechanism occurs when a particle with keen edge indents deeply on the target surface then ploughing is said to be occurs.

Cutting the cutting of surface occurs, when a particle impacts at lower angle.

Sliding This includes the sliding of a particle on the material surface which leads to sliding crater.

- **Mechanism for Brittle Material**

There are two different erosion mechanism recognised for brittle materials as listed below-

Indentation

This type of fracture is observed for brittle materials a high flow velocity. Since at higher flow velocity, the impacting load also becomes high which results in high stress at the surface of target component. Due to which there will be evolution and propagation of radial and lateral cracks.

Chipping mechanism

Whenever keen edged solid erodent/particles are present in the flow then a mechanism might occur which includes the formation and propagation of crack. For instance, the chipping mechanism is generally observed on the surface of boron carbide surfaces when sharp edged particles are present in the flow.

1.7 Types of Erosion Wear

Particulate erosion- in this type of erosion wear solid entrained in the fluid hits the wall of the pipe line and removes considerable material. It is the Most common erosion wear that is observed in industry

- Liquid droplet erosion
- Erosion-Corrosion
- Cavitation

1.8 Dependency of Particulate Erosion Wear

Erosion wear is a complex phenomenon which depends on many parameters, such as:

- **Particle properties**
  - Shape
  - Size
  - Density
  - Concentration
- **Particle tracks**
- **Local flow and turbulence field**
- **Surface condition**
- **Effect of cavities produced after material removal**

1.9 Particulate Erosion in Industry

The process of wear in which material gets extracted from a component's surface by the repeated hitting of the solid erodent entrained in the moving fluid. In industry particulate erosion are associated to constructive and destructive process. Erosion wear is quite often observed in the process or industry listed below:

- Oil and Gas Industry
- Abrasive jet micro machining
- Slurry transport
- Mining
- Chemical Industry
- Blast machining
- Abrasive jet machining
- Turbine blades in power generating plants
- Heat exchanger

There are three scientific methods to predict the effect of erosion wear. The most common method is physical testing which includes several experiments under specific conditions to observe the erosion wear. It is very time consuming and subjected to lots of error and trial. Second method includes developing some numerical models which includes deriving of equations to forecast the erosion wear. The last method used computer based simulations to obtain the solution of erosion wear virtually.

1.10 Motivation for the Work

The conveyance of Bottom ash-Water slurry from the generation unit to disposal well through transporting pipe line is always subjected to some kind of wear of the industrial systems. This wear is capable to degrade the pipe material and may results in reduced productivity. It is also a concern of safety too. So a proper design of the pipe line is must to safely transport the slurry. The aim of this work is to study the erosion wear by using CFD techniques by which prediction the erosion wear of a pipe line can be done at different operating conditions like flow velocity, pipe diameter, bending ratio, bending angles etc. The developed model can be applied to predict erosion wear of industrial systems with the flow of solid-liquid mixture

CHAPTER 2

LITERATURE REVIEW

Badr et al. (2002) performed the erosion wear simulation study of a carbon steel sudden contraction pipe having contraction ratio of 2:1 using Computational Fluid Dynamics (CFD) code FLUENT. They evaluated the influence of velocity and particle diameter on erosion wear caused by solid-liquid slurry. Sand particles having several sizes (10-400 μm) were simulated at different velocity, ranging from 1-10 m/s. It was observed that the particles were creating more impact on the contraction plate while their impact on the wall was comparatively insignificant. The smaller sized particles of 10 μm showed negligible erosion wear at exit of annular plate and achieved maximum magnitude near entrance of smaller pipe. The maximum and minimum erosion rates were observed at flow velocity of 10 and 1 m/s respectively.

Bozzini et al. (2003) studied erosion wear of 90^0 pipe bend for different flow conditions of multiphase regime. Experimental and computational analysis was formed. The simulation study was carried out by using CFD code FLUENT with Discrete Phase Model (DPM). The multiphase flow was comprised of sand particles of 300 μm size and air with velocity 2 to 10 m/s. Results showed that at lower velocities, the erosion rate was observed due gravitational settling of the particles while drag force was responsible for at higher velocity. At higher gas concentration, more damage was encountered at the bottom of the first half of the bend.

Chen et al. (2004) reported a simulation study to analyse erosion wear for aluminium an elbow and a plug tee. The CFD code CFX was applied with the k-ϵ turbulence modeling scheme to solve the multiphase flow of sand-air. The sand particles of 150 μm diameter and air with velocity in range of 15 - 45 m/s were considered for the simulation. For higher accuracy of results, grid and particle independence test was performed. To observe the particle-wall collision efficiently, two wall collision model as stochastic and forder rebound were used. The results from the stochastic model have a better agreement with the experimental results while the forder model showed approximately 15% high erosion than the experimental results. The erosion location for both the pipelines was also traced by using graphical approach.

Habib et al. (2007) studied influence of impact velocity, particle size and concentration on the erosion wear for pipe section having sudden contraction. The simulation study was performed at different flow velocity within the range of 1-10 m/s, particle concentration 2-10% and particles size of 10-400μm. Commercial CFD code FLUENT with DPM to track the particles with K-ϵ RNG turbulence modeling scheme was used solved by using. They observed that impact of particles was significant on contraction plate and insignificant on pipe wall. It was found that the particles with higher size were highly capable to erode more material and 1.1 times increment in erosion rate was noticed as particle diameter changed from 100 μm to 200μm. This increasing behaviour continues up to a certain particle size of 300 μm. The effect of particle size on erosion rate becomes insignificant above 300 μm.

Patil et al. (2011) conducted an experimental study to evaluate the influence of operating parameters on the erosion wear triggered by the collision of solid liquid mixture on the aluminium sheet. The particle size was varied from 225-885 with concentration ranging from 10-20%. The particles were injected on the sheet surface at different angles from 15-90^0 at velocity variation of 3.6-9.6 m/s. They reported that the maximum erosion occurs at 45^0 impact angle and starts to decrease till impact angle reaches to 90^0. A linear increment in the erosion rate was noticed with particle size and flow velocity. Velocity was the found to be the most dominating factor among other parameters. A correlation was developed on the basis of experimental results which was capable to predict erosion wear at different operating conditions.

Zhang et al. (2011) performed a simulation study to investigate the erosion wear in a 1.6 m long elbow having a density of 2960 kg/m^3. To account the effect of particle trajectory and inter particle interaction the Discrete Element Method (DEM) was applied in CFD code FLUENT. The solution of fluid phase was obtained by volume averaged N-S equation. In this work the influence of velocity, bend geometry and orientation on erosion wear location was analysed. It was observed that, the location of maximum wear was not affected by slurry velocity. The maximum erosion location reported for u-shaped pipe was found to be quite similar with 90^0 pipe bend while it was appeared to be different when the bend orientation was changed.

M.M. Stack et al. (2011) developed a model to investigate the influence of particle contamination on erosion-corrosion of a 0.078 m diameter standard pipe bend. A 3-D

mapping technique was used to track the solid concentration. The slurry of water and alumina particles were simulated at a flow rate of 14.3 kg/s at different volume fraction in the range of 0.025 to 0.1. CFD code FLUENT with k-ω model was used to solve the flow. The results stated that the occurrence of erosion-corrosion was mainly found at the bend region. Higher particle concentration tends to erode more material due to the reduction in impact time of particle.

Okita et al. (2012) reported a study to analyse erosion wear for an aluminium Al6061-T6 alloy under different operating conditions of fluid viscosity. Carboxyl Methyl Cellulose (CMC) was mixed with water at different concentration to form fluid of different viscosity. The flow was studied at different viscosity in range from 1 to 50 centi poise at variable particle size of 20 to 150 μm. The computational part was performed by using CFD code FLUENT 6.3. The experimental results were also compared with the CFD predictions. The value of erosion rate was found to be decreased at more viscous flow. At 10 cp viscosity, the erosion rate caused by 20 μm sized particle was found to be 50% more than 150 μm sized particles. The results stated 2 times decrement in erosion ratio when the viscosity of fluid was changed from 10 to 30 cp.

Njobuenwu et al. (2012)[4][4] conducted a study to analyse the erosion wear on 90^0 square bend having different r/D ratios in range of 6-10. In this investigation five different erosion models were applied to predict the erosion wear. The developed model so developed that it can predict the erosion on both the concave and convex region of the pipe bend. The maximum erosion was reported on the concave wall of bend entrance. A weak secondary erosion depth was also observed at the concave wall of bend outlet. The interaction of the wall and particle was neglected in this study.

Deng et al. (2013) performed a computational analysis of erosion wear in a 50 mm diameter 90^0 elbow. The simulation study was carried out by using CFD code FLUENT along with DPM and standard k-ϵ turbulence modeling. The carrier fluid was air having a velocity of 30 m/s. The solid particle with different size in range of 10-400 μm at mass loadings variation from 0.2-0.10 was simulated for distinct pipe curvature ratio (r/D) in range of 1.5-7.8. The comparison of erosion wear for pipe bend and plugged tee was also performed. It was observed that the larger sized particles erode more material due to their high inertia. The

results showed low erosion for high curvature ratio pipe lines. The erosion in plugged tee was about 70% of pipe bend at the same operating conditions.

Wu et al. (2013) reported a simulation analysis of erosion wear for industrial pipe lines by using CFD code Fluent with DPM and k-ϵ model turbulence modeling scheme. In this study pipe bends with different r/D ratio in range of 2 to 10 and sudden expansion pipes with expansion ratios varying from 1.4 to 2.0 were considered. The multiphase flow of oil and sand at 0.5% concentration were simulated. For pipe bends erosion damage was majorly reported at 30^0 and 45^0 of the bend. The least value of pressure was found at the sudden expansion part of expansion pipe while the region of maximum erosion was reported at just after the expansion zone. Particle with an impact angle of 80-90^0 causes severe erosion in pipe bend while effect of impact angle was very less for the straight pipe.

Zhang et al. (2013) developed a probability model to predict the erosion caused by solid particle in a straight pipe line. CFD code Fluent with two equation k-ϵ turbulence modeling scheme was applied to account the turbulence of flow. Investigations were performed at various particle size in range of 50-400 μm at different velocity from 3.048-15.240 m/s. The pipe diameter was also varied from 50.5 to 203.2 mm to obtain their effect on erosion wear. The model was then verified with the experimental findings. The results showed that increase in particle size causes more erosion up to a certain extent after then the increment was limited. The pipe diameter was found to have an inverse relation with the erosion rate as the large diameter pipe suffered with low erosion. Erosion rate was increased to 6.4 times when the velocity shift from 3.048 to 6.096 m/s.

Abdolkarimi et al. (2013) developed a model to find out the erosive effect of particles on industrial pipe lines by using CFD. A Lagrangian approach was used to solve the solid-gas flow at a flow velocity of 20 m/s through a 90^0 pipe bend of 56 inch diameter. The particle motion was analysed by using CFD code FLUENT and it was noticed that the bigger sized particles move towards the outer region of the pipe line thus creates more erosion there. The radial velocity profile of gas and particles were found to exist in different planes. The location of maximum wear was reported to be concentrated in between 40 to 65^0 of the bend curvature. The results were validated with the experimental data and were found to be quite acceptable with them.

Macchini et al. (2013) proposed a study of erosion wear on pipe bend of pneumatic conveyors. In this work investigations were carried out to find out the effect of various parameters on erosion rate such as particle concentration, particle size and density. The mild steel pipe has a diameter of 102 mm and r/D ratio of 3. Wood dust, olivine sand and the silica flour were used as erosive materials. The experimentation was conducted at two different velocities of 17 and 45 m/s. The volumetric concentration of the particle was varied from 0.001 to 0.020. Result showed low erosion rate at high particle concentration as at higher concentration the inter particle collision gets increased which results in less chances of erodent-wall collision. It was also observed that the erodent with high density (silica flour 2690 kg/m^3) caused 20 times more erosion than lower density erodent (wood dust 443 kg/m^3).

Safaei et al. 2014 investigated the influence of particle size on the erosion wear of 90^0 pipe bend. Simulation study was performed for the multiphase flow of water and copper particle. The size of the copper particle was varied from 10 nm to 100 μm at three different velocities in range of 5-20 m/s. The commercial CFD code FLUENT along with Lagrange particle tracking and standard k-ϵ modeling scheme was applied for the simulations. The result stated that erosion rate caused by micro size particles was many times more than nano sized particles. A threshold velocity was identified below which the influence of particle size on erosion rate was insignificant. The impact of velocity on erosion rate was found to be more adverse than other parameters. For the same concentration, the erosion caused by a 20 m/s velocity was 7.5 times higher than that 10 m/s.

Mansouri et al. (2014) conducted experimental and computational study to observe the erosion wear of a target sheet caused by water-sand and air-sand multiphase. To account the turbulence of flowing fluid a SST k-ϵ with the particle tracking scheme was used in FLUENT. The CFD results showed a deviated path of the sand particles for air-water multiphase while a parallel path was observed for air-sand flow. Two different profile of erosion wear as W and U-shape was generated on the sheet wall for solid-liquid and air-solid flow respectively.

Zeng et al. (2014) performed experimental and numerical analysis of erosion-corrosion on carbon steel pipe bend. In this study CFD code FLUENT was applied along with standard k-ϵ turbulence model. The DPM model was selected for the analysis of multiphase flow while a

single phase model was also applied to study the effect of secondary flow. The results stated that the sand particle was highly concentrated at inner region of upper straight pipe resulted in higher erosion at that region. Erosion magnitude and sand concentration were found to be shifted from the inner to outer wall along the elbow curve. The particles were found to create impact on the elbow wall under the inertial, drag and secondary flow effect.

Sahata et al. (2014) proposed a study to analyse erosion wear in 90^0 elbow for different flow rates and particle concentrations. The simulation analysis were performed by using CFD code FLUENT with DPM model and standard k-ω turbulence modeling scheme. The particle concentration was varied from 1-11 grams/litre and Reynolds number from 580 to 26000. The location of maximum wear was also reported. An increased erosion rate was observed when the flow rate and the particle size were increased. The location of maximum wear was found to be different for different flow conditions. The model was validated with the previous year experimental work of three authors which showed good agreement with them.

Hadziahmetovic et al. (2014) developed a model to predict erosion wear caused by the multiphase flow of air and sand particles on a 25.4 mm diameter elbow. The work was based on computational technique and performed by using commercial CFD code FLUENT. To study the particle motion and particle-wall interaction correctly, two different models were applied as deterministic model and stochastic rebound. Two different planes were considered for the simulations, the first plane was 100 mm below the elbow while the second plane was 100 mm ahead the elbow. Air was made to flow with velocity of 45.72 m/s from inlet of the elbow. The outcomes of the simulations were verified with the previous experimental data. The obtained results by stochastic model showed better agreement with the previous published data than the deterministic model.

Jafari et al. (2014) observed the consequence of wall roughness on the erosion wear for the sudden contraction pipe. In this work the multiphase flow of solid with 100 and 200 μm size and gas with 10 and 15 m/s velocity was simulated. The findings of the CFD simulations were also compared with the previous published data. It was found that for rough pipe wall the particles was majorly concentrated near the inner region of the wall causing more erosion there by more frequent collision. It was also reported that erosion wear for the annular pipe

was found to be more significant at wall extrodes than ordinary pipe of same radius. More erosion wear was found with increased radius ratio.

Solonordal et al. (2015) used experimental and computational analysis to observe the erosion wear caused by sand particle in a standard 90^0 elbow. Sand particles of 184 µm size along with air of velocity of 80 m/s was made to flow through the pipe line. For computational analysis ANSYS code CFX 15.0 was adopted with Finnie erosion model in conjunction with k-ϵ SST turbulence modeling. The effect of pipe wall surface condition on erosion wear was studied by considering smooth and rough wall. It was found that CFD simulations for a smooth pipe resulted in a v-shaped erosion profile and predicts almost 4 times higher erosion rate than the experimental results. This variation might raised due to the particle-particle interaction which was not considered in the smooth wall simulation. Somerfield particle collision model was adopted in the simulation for rough pipe and the obtained result were quite similar with the experiment.

Shamshirband et al. (2015) investigated the effect of particle size on the erosive wear of a 90^0 pipe bend by using CFD code Fluent. They used Std. k-ϵ turbulence modeling scheme and DPM to track the movement of the particles. The diameter and length of the pipe was 3.5 mm of 70 mm respectively. Copper particles were used as erodent in the study. The particle size was varied from 10 nm to 100 µm at three different velocities which were in the range of 5-20 m/s. The result outcomes showed that the maximum erosion caused by micro size particle was found to be several times higher than the nano sized particles. At fixed particle concentration of 4%, 9.5 times increment in erosion rate was reported when the velocity shifted from 10 m/s to 20 m/s.

Lopez et al. (2015) applied jet impingement technique to evaluate the erosion wear on a target plate by using two different simulation methodologies i.e. ANSYS code FLUENT and OpenFoam 2.2x. In this analysis, the distance between nozzle and target was kept as 5 and 25 mm respectively. The density of sand particles for 5 and 25 mm distance setup was 2206 and 2300 kg/m^3.and Discrete random walk model and stochastic dispersion was used for FLUENT and OpenFoam respectively. Results obtained by both of the methodology was compared with each other. The mean velocity difference for FLUENT and OpenFoam was 2% while the angle of impingement had a difference of 15.3%.

Khan et al. (2015) carried out an experimental investigation to find out the influence of slurry concentration on the erosion behaviour of a mild steel pipe. The concentration of the slurry was varied from 20 to 60%. SEM images of the mild steel pipe were also taken before and after the erosion test. The obtained results stated that the erosion rate increases till the slurry concentration was increased from 10 to 40%, furthermore increment in concentration showed decrement in the erosion growth. Such behaviour was observed due to more particle-particle interaction at higher concentration.

Duarte et al. (2015) performed a computational and experimental investigation on erosion behaviour of a 254 mm diameter 90^0 pipe bend. The sand particles were simulated at different mass loading in the range of 0.013-1.5 kg_p/kg_g by using one way, two way and four way couplings. The results by all couplings at low concentration showed same erosion contours while different contours were obtained by using higher sand concentration. The maximum erosion was predicted by four-way coupling. It was also noticed that by increasing the particle concentration the inter-particle collision increases which reduces the erosion magnitude.

Chen et al. 2015 developed a solid-liquid two phase erosion model for elbows. The proposed model takes into consideration the interaction of liquid-solid, solid-solid and solid-wall. The sand and water multiphase was simulated at a velocity of 3 m/s. The sand particles were having a size of 150 μm and density of 2650 kg m^{-3}.They have used Hertz-Mindlin no slip model for solid-solid and solid-wall contact. Maximum erosion rate and their location in three different elbows (90^0,60^0 and 45^0) of diameter 40 mm were investigated. The maximum erosion rate for a 60^0 elbow was found to be 3.45×10^{-19} kg m^{-2s-1}. Investigations show that maximum erosion locations for different elbows were mostly near at the exit of bend and also the maximum erosion rate increases with large bend angle.

Peng et al. (2016) performed a CFD based study to simulate erosion wear for the multiphase flow of solid-liquid in 90^0 pipe bend. The diameter of the mild steel pipe was 50 mm. The work was performed using commercial CFD code FLUENT. A two way coupled model based on Euler-Langrage approach with Standard k-ϵ model was adopted to solve the multiphase flow in this work. The influence of velocity, particle diameter, particle mass flow and pipe diameter on the erosive wear of pipe bend was investigated. A relationship between

the stokes number and location of maximum erosion was also reported. Excluding the pipe diameter, all of the other parameters showed enhancement in erosion rate while pipe diameter has an inverse relationship with erosion rate. It was also found that the maximum erosion rate occurs at the inner side of wall for less stokes number while higher stokes number creates maximum erosion at the outer most side of the wall.

CHAPTER 3

MULTIPHASE MODELING OF EROSION WEAR

Multiphase flow is simply a combination of phases like solid-liquid phase, liquid-gas phase, solid-gas phase and such similar flows. As Multiphase flow is a combination of phases, then the main of primary phase is treated as continuum and the other phases are considered to be dispersed phases. Most of the engineering and industrial applications like chemical reactors, power generation, oil and gas production involve the multiphase flow regimes in them. The study of multiphase flow is a complicated problem that includes the investigation of fluid mechanics, heat exchange, mass exchange, energy exchange.

3.1 Classification of Multiphase flow

According to the state of different phases multiphase flow can be classified as:

1. Liquid-Liquid or liquid gas flows
2. Liquid-Solid flows
3. Gas-Solid flows
4. Three phase flows

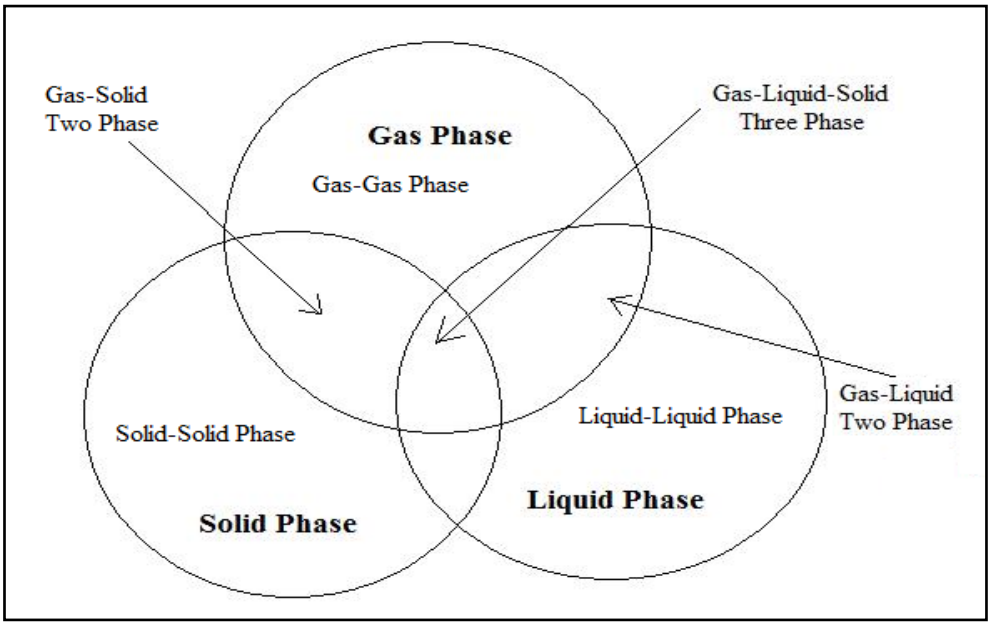

Figure 3.1: Classification of multiphase flow

Furthermore, experiments on multiphase flow are difficult to conduct. The evolution of computational fluid dynamics (CFD) is found to be very useful in simulating such flow. The Multiphase models in CFD are generally based on Euler-Euler approach and Euler-Lagrange approach.

3.2 Approaches for Multiphase Modeling in CFD

The most common approach in CFD codes for solving the multiphase flow are:

3.3.1. Euler-Lagrange Approach

3.3.2. Euler-Euler Approach

3.2.1 Euler-Lagrange Approach

In this approach the fluid is treated as a continuous phase and its solution is obtained by solving the Time Average Navier-Stokes equations. The solution of dispersed phase is obtained by tracking the number of particles or droplets trajectory along the flow. The secondary dispersed phase applies an effect on the continuous phase though a force. There is a exchange of mass, momentum and energy between the continuous phase and dispersed phase. One of the assumptions of this model is that low volume fraction is occupied by the secondary phase or dispersed phase, though large mass loading is also acceptable. This approach is found to be suitable for the modeling of particle-laden regimes, spray dryers and coal-liquid fuel combustion

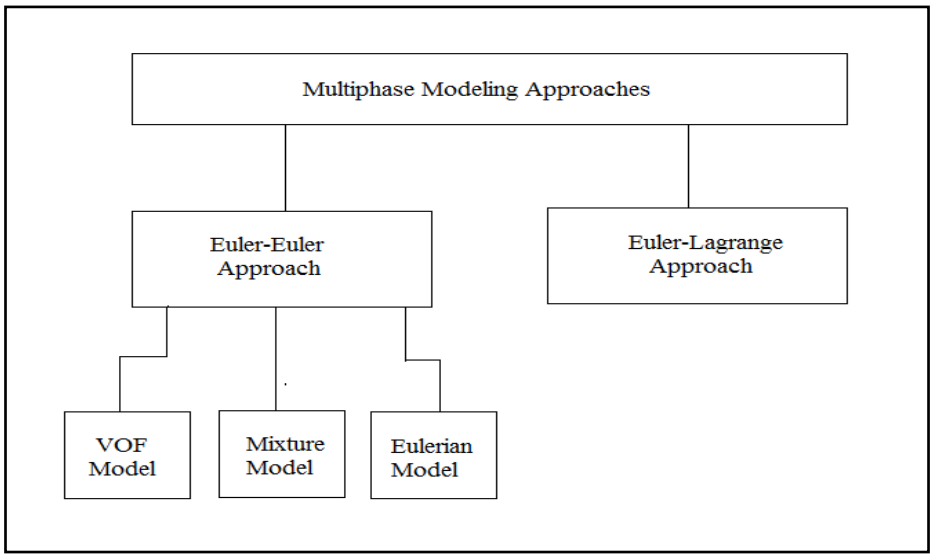

Figure 3.2: Different multiphase modeling approaches

3.3.2 Euler-Euler Approach

Euler-Euler approach is an approach which can numerically simulate the continuous phase and dispersed phase. This approach treats each phase as a continuous phase and the

conservation equations are applied to each of the phases to derive set of equation. The fraction of volume for each phase is introduced and is considered as continuous function of space and time. The addition of the volume fraction must be equals to one. The different Euler-Euler models available in CFD-FLUENT are Volume of Fraction (VOF), Mixture model and Eulerian model.

1. VOF Model- This model was developed for two or more insoluble fluids. In this model, a single or common set of momentum equation is shared by different phases. This model is often implemented for stratified flow, large size bubble motion in liquid, predicting the breakup of jet etc.

2. Mixture Model- Mixture Model is used for two or more phases having an assumption of same velocity for secondary phase. This model solves the momentum equation for the mixture. This model can be applied to the bubbly flow, cyclone separator, particle laden flow. It is widely used for the flow having solid and liquid phases.

3. Eulerian Model- This model is considered to be the most complex amongst the all multiphase model in FLUENT. In this model n number of momentum and continuity equations is solved for each of the phase. In this the continuous phase is treated first and after that solid phase is treated. This model is best suited to the flow having particle suspension, bubbles and also for fluidised beds.

3.3 Multiphase Model Formulation

In this study the Euler-Lagrange two phase model was implemented, whereby solid phase is considered as discrete phase and allows particle tracking for it. While the liquid phase or primary phase is treated as continuous phase and its solution is obtained by time averaged N-S equation. The discrete phase applies an effect on continuous phase by a force applied at dispersed phase. In the present CFD work the Euler-Lagrange multiphase modeling approach was applied in FLUENT 15.0.

3.3.1 Conservation Equation

Mass Conservation Equation

The generalised equation for the mass conservation can be demonstrated by mass balance equation and can be written as:

$$\frac{\partial}{\partial t}(\rho_n + \alpha_n) + \nabla.(\rho_n \alpha_n V_n) = 0 \quad (3.1)$$

Here the first and second term denotes the rate of density change with respect to time and the net flow rate of mass coming out of the fluid element respectively. α, n and ∇ denotes volume fraction, number of phase and the partial derivatives with respect to all directions respectively. The addition of α_n must be 1.

$$\sum_n \alpha_n = \alpha_l + \alpha_g + \alpha_s = 1 \quad (3.2)$$

Momentum Conservation Equation

The generalised equation for the momentum conservation demonstrates that the change in rate of momentum:

$$\frac{\partial}{\partial t}(\rho_n \alpha_n V_n) = +\nabla.(\rho_n \alpha_n V_n) = -\alpha_n \nabla P + \nabla.[\alpha_n(\tau_n + \tau_n^t)] + \rho_n \alpha_n g + M_i \quad (3.3)$$

$$\nabla.[\alpha_n(\tau_n + \tau_n^t)] = \nabla.[\alpha_n \mu_i(\nabla V_i + ((\nabla V_i)^T)] \quad (3.4)$$

Here, α and n denotes the volume fraction and the phase number respectively. The addition of α_n must be 1, p τ_n, τ_n^t and M_i denotes the pressure with the assumption of having same value in all phases, molecular stress, turbulent stress, and the momentum exchange between the phases respectively.

The combination of mass and momentum conservations are called as Navier-Stoke equation.

Energy Conservation Equation

The generalised form of energy conservation is based on the 1st law of Thermodynamics which tells that the change in energy of the fluid particle is equal to the summation of the heat supplied to the fluid particle and work done on the particle, it can be represented as:

$$\frac{\partial}{\partial t}(\rho E) + \nabla.(V(\rho E + p)) = -\nabla.\sum_j h_j j_j \quad (3.5)$$

3.4 Turbulence Modeling

Solving multiphase stream is extremely complicated. Variations in the flow velocity will cause change in the momentum and energy of the transported fluid. Moreover during

performing a numerical study, the computer capacity and time are the important factors which affect the multiphase solution. This has prompted the execution of models that can solve various levels of physics, involving distinctive levels of precision and proper for various multiphase stream applications. Not a single turbulence model is universally applicable for all types of conditions. Depending upon the flow conditions, wisely selection of turbulent model amongst the various available models is must. The available turbulent modeling schemes are illustrated in figure 3.3:

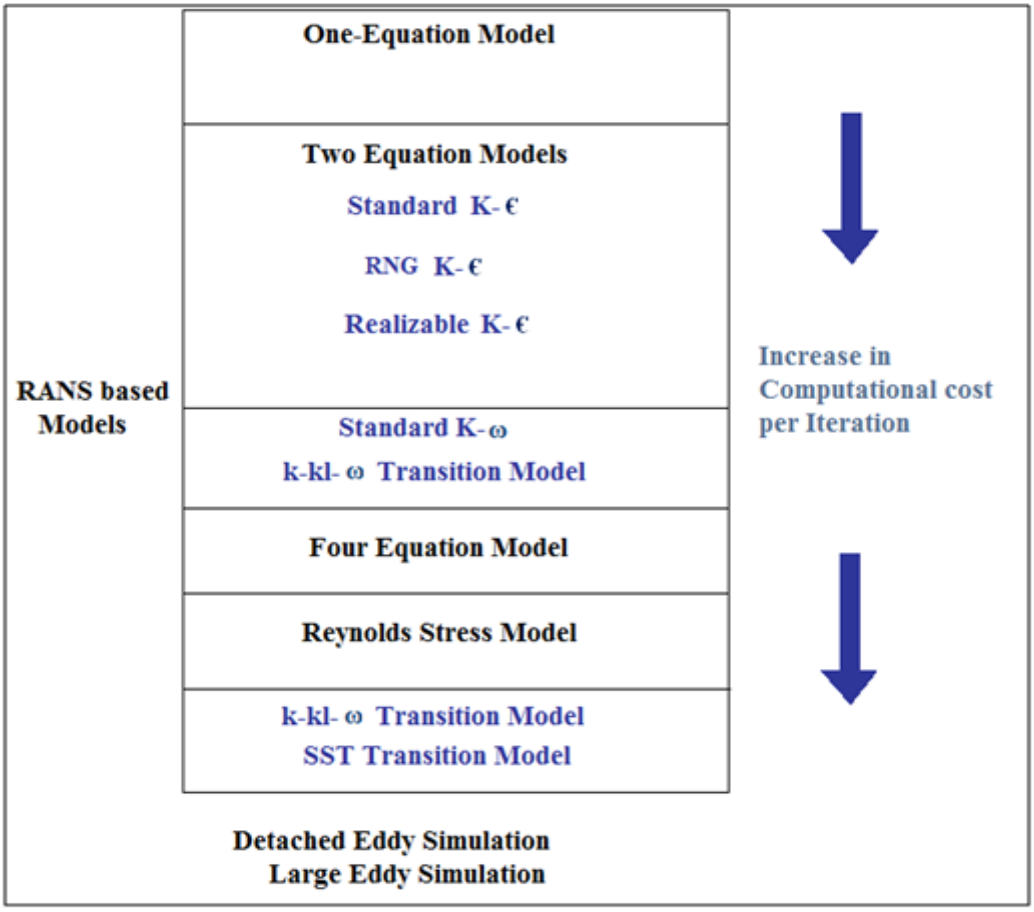

Figure 3.3: Different turbulence model

3.4.1 RANS Based Turbulence Models

One Equation Model:

Spalart-Allamaras: It is a low cost RANS model can be used to solve the modified eddy viscosity transport equation. It is mainly applied for aerodynamic and turbo machinery applications having slight separation

Two Equation Models-:

k- ϵ Models They are the most widely utilized turbulence models as it conveys economy and reasonable exactness for a broad variety of turbulent streams.

This model is again divided into three distinct categories as:
Standard k-ϵ
Realizable k- ϵ
RNG k- ϵ

Standard k-ϵ Model: It is the widely used and most popular model to solve the turbulence flow of industrial applications. It is robust and sensibly exact for variety of applications. K stands for the kinetic energy and ε stands for turbulent dissipation rate. It also has sub models for buoyancy, compressibility etc.

Realizable k- ϵ Model: It can be said as the improvement of the standard k- This models provides better prediction for both the planar and round jets, it also gives supreme results for rotational flows, separation and recirculation.

RNG k- ϵ Model: This model provides better prediction for rotational flows, separation and recirculation.

k- ω Models k-ω model is the widely preferred model to account near wall treatment. It is comparatively precise, resilient and more stable. Its sensitivity to inlet stream turbulence is considered as its disadvantage. They are further divided as:

Standard k-ω Model
SST k-ω Model

Standard k-ω Model: This model is used to account the complexity of the turbulence flow near the wall. It also gives better prediction for the flows that involves separation and high pressure difference. This model is excessively adopted in aerospace and turbo machinery.

SST k- ω Model: This model is a hybrid one, which includes both the benefits of both the previous discussed models that is near wall treatment of k- ω and outer portion of boundary layer of k- ϵ. It includes the feature to form advanced wall which reduced the dependence of the result on the mesh refinement on wall.

3.4.2 Reynolds Stress Model

This model is mostly used for 3D flows and anisotropic flows. The cost of computation is higher as compared to the above discussed models. This model is quite tougher to converge. It is best suitable for flow involving swirl, flow of cyclones, combustors having swirl, curvature.

3.5 Turbulent Model Formulation

To obtain the solution of the turbulence of the multiphase flow, a Standard k$-\epsilon$ model was implemented in the present CFD work.

Equation for turbulent kinetic energy transport-

$$\frac{\partial \rho k}{\partial t} + \nabla.(\rho \vec{v} k) = \nabla.[\left(\mu + \frac{\mu_t}{\sigma_k}\right)\nabla k + G_k - \rho \epsilon \quad (3.6)$$

Equation for dissipation of turbulent kinetic energy transport-

$$\frac{\partial \rho\, \epsilon}{\partial t} + \nabla.(\rho \vec{v} \epsilon) = \nabla.[\left(\mu + \frac{\mu_t}{\sigma_\epsilon}\right)\nabla \epsilon + \frac{\epsilon}{k}(C_{\epsilon 1} G_k - \rho \epsilon C_{\epsilon 2}) \quad (3.7)$$

The constant presented in this model $C_{\epsilon 1}, C_{\epsilon 1}, \sigma_k, \sigma_\epsilon$ have the values as listed in table

Table 3.1: default value of coefficient for k-ϵ Standard Model

$C_{\epsilon 1}$	$C_{\epsilon 2}$	σ_k	σ_ϵ
1.44	1.92	1	1.3

3.5.1Turbulence Equation

The turbulence is solved by using the standard k-ϵ model. The equation is in the form:

$$\nabla.(\rho u \varphi) - \nabla.\frac{\mu_{\text{eff}}}{\sigma_\varphi} = S_\varphi \quad (3.8)$$

Here φ represents k or ϵ, σ_φ represents the turbulent diffusivity of φ andS_φ.

3.6 Erosion Model

The erosion rate caused by solid particle can be written as:

$$\text{Rerosion} = \sum_{p=1}^{N\ particl\ es} \frac{(\mathrm{m_p C(d_p)) f(a) V^{b(v)}}}{\mathrm{A_f}} \quad (3.9)$$

The calculation of erosion through equation (3.13) is expressed as amount of material removed per unit area and time.

The default values for the constants are as: C=1.8×10^{-9}, $b = 0$ and $f = 1$.

m_p: Mass flow rate of the particles

f (a): Impact angle function

V: Particle impact velocity

B (v): Velocity exponent

C (d_p): Particle diameter function

The Value of C is 1.8e-09 is set as default.

Theory of Particle Motion

- **Particle Force Balance**

The Particle Trajectory is predicted by FLUENT by integrating the force balance on particle. In the force balance the particle inertia is equated to the forces applied on the particles as:

$$\frac{du_p}{dt} = F_D\left(V_f - V_p\right) + \frac{g(\rho_p - \rho_f)}{\rho_p} + F\ . \quad (3.10)$$

Where F= Force. Here the force consists of two terms a drag force and a buoyancy force.

The drag force applied to the particle can be written as:

$$F_D = \frac{18\mu}{\rho_p d_p^2} + \frac{C_D R_e}{24} \quad (3.11)$$

Where, C_D is the drag coefficient which can be written as:

$$C_D = a_1 + \frac{a_2}{Re} + \frac{a_3}{Re} \quad (3.11)$$

And, Re is the particle Reynolds number which can be written as:

$$Re = \frac{(\rho d_p |\vec{V}_p - \vec{V}|)}{\mu} \quad (3.12)$$

- **Particle Turbulent Dispersion**

To predict the turbulence of the particles present in the flowing fluid, stochastic tracking of particle and cloud model are available in FLUENT. Stochastic tracking accounts the influence of instantaneous velocity fluctuations on the trajectories of particles. While the tracking of particle cloud at its mean trajectory is evaluated by particle cloud model.

Stochastic Tracking

In the turbulent stream, the particle trajectory is predicted by considering the mean phase of flow velocity ($\bar{u}$). The dispersion effect of particle caused by the turbulence of flow can be predicted by using fluctuating component of fluid velocity as:

$$u_f = u_f^1 + \bar{\bar{u}}_f \quad (3.13)$$

In this approach, the prediction of particle tracks by FLUENT is by integrating equation of trajectory for every single particles by considering the instantaneous velocity $u_f^1 + \bar{\bar{u}}_f(t)$.

Particle Cloud Tracking

The dispersion of particles due to turbulence of the flow will also predicted by using particle cloud model. The tracking of particle cloud at its mean trajectory is evaluated by this model. This model uses Gaussian probability density function (PDF) [ ] and its variance depends on the extents of particle dispersion caused by the turbulence variations.

3.7 Components of Erosion Modeling

Particulate erosion involves the flow of primary phase (mainly water) and secondary phase (erodent/solid phase). It is very necessary to accurately analyse both the phases and also the relation existing between them. The relationship between fluid and particles are analysed by considering couplings (one way, two way and four way coupling). Many things are

considered in erosion modeling set up like particle-fluid interaction, particle-wall interaction, particle motion etc. The main components of erosion modeling are shown in figure 3.4.

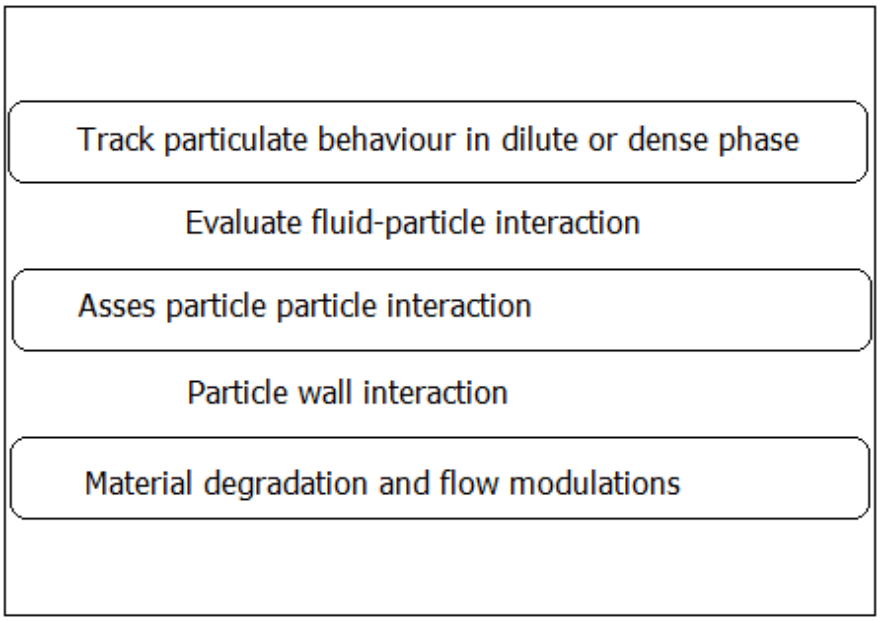

Figure 3.4: Various components of erosion modeling

Types of Particles in FLUENT

Several types of particles are observed in industrial applications. To account the effect of such a variety of particles, FLUENT has categorized particles into different groups. Table 3.2 shows types of particles along with their descriptions. We can choose any particles from the injection panel of FLUENT. Each group of particles have their pre-specified law, additionally some user defined laws can also be implemented in them.

Table 3.2 Types of particles available in FLUENT

Types of Particles	Description
Inert	Inert
Droplet	Heating/Evaporation/Boiling

Combusting	Heating
Multi-component	Multi-components droplets/particles

3.9 Previous Researches on Pipe Erosion Using CFD

Several researches were performed to observe the erosion wear of slurry pipe line for multiphase flow of solid liquid. Erosion wear is a complicated phenomenon which depends on many factors. Various author uses Computational techniques to evaluate the effect of operating conditions on the erosion wear of pipe line. Table 3.3 below shows the brief details of the previous studies in which CFD was used to examine the erosion wear.

Table 3.3: Previous studies on Erosion Wear using CFD

Author	**Code, Turbulence scheme, Mesh, Convergence**	**Particle Material /(Density) [kg/m^3]**	**Particle Conc, size[µm]**	**Flowing Fluid Type/ Velocity [m/s]**	**Pipe Material/ (Density) [kg/m^3]**	**Findings**
Safaei et al.[2014]	CFD-FLUENT k-ϵ (Std) Hexahedral, 0.000001	Copper	0-4%, 10-100 µm also 10-100 nm	Dilute water, 5,10,20	Pipe bend, 0.016 m long, Aluminium 3003 alloy	Large sized particle causes more erosion. An increment of 7.5 times in erosion rate was found when velocity shifts from 10 to 20 m/s.
Jafari et al. [2014]	CFD k-ϵ(std)	1000	Mass ratio 0.4, 0.9, 1.1, 100 µm and 200	Gas, 10 and 15	Brass, horizontal pipe, 30 mm dia.	More erosion was observed for rough pipe. Pipe with large radius ratio suffers with

			µm			more erosion.
Duarte et al.[2015]	UNSCYFL 3D k-ϵ Tetrahedral	Angular SiO_2 (2600)	Mass loading (0.013, 0.25, 0.5, 1.0, 1.5), 182 µm	Air, 34.1	Aluminium 6061-T6 (2700), pipe dia-0.0254m	At low mass loadings, magnitude of erosion wear obtained by all the couplings was almost same. Higher mass loadings give more erosion at four way coupled models.
Solnordal et al.[2015]	CFD-CFX k-ϵ(SST) unstructured	Sand (2650)	1.76*10-5 (volume fraction), 184 µm	Air, 80	steel, pipe-bend(vertical) 102.5mm diameter	The CFD results of rough pipe gives realistic erosion, while the results of smooth pipe give almost four times higher erosion than the experimental findings.

Chen et al.[2015]	CFD-FLUENT-DEM k-ϵ (Std)	Sand (2650)	Sand, 150 µm	Water, 3	pipe-bend (45^0,60^0 and 90^0) 40 mm dia, 10d length	The highest magnitude of erosion rate was observed for 600 pipe bend. The location of maximum wear was almost same for all the bends and is located at the exit zone of pipe.
Pereira et al. 2014	CFD-FLUENT DPM Hexahedral		0.0042%, 150 µm	Air, 45.72	Aluminium, Pipe bend	Four different erosion model was applied in this work. The results obtained from zhang and oka erosion model gives closer result to the experimental result.
WU et al. 2013	CFD-FLUENT k-ϵ (Std) DPM	Sand (2650)	0.5%, 250 µm	Oil, 3	bend and sudden expansion	Impact angle from 80^0-90^0 eroded more material in pipe bends while their effects on straight pipe are negligible. The maximum erosion wear location for pipe bend was near to the 30^0 and 45^0 of bend.
Zeng et al. 2014	CFD-Fluent k-ϵ (STD) DPM, 0.000001	Sand	11.2 %, 300-400 µm	4	Mild-steel, Bend	The sand particles were highly concentrated at the inner side of the up-straight pipe due to which the region magnitude was also high at this region. The particles are impacting the elbow under the influence of inertial, drag and secondary flow effect.

Mansouri et al.[2014]	CFD-FLUENT k-ϵ DPM	Sand (2650)	300 µm	Water and Air, 72,109 for air and 23 and 35 for water	stainless steel-316 (2700)	The particles track shows deviated path for solid-liquid flow while parallel path for the solid-air flow. A W-shaped erosion profile was generated on the target by solid-liquid stream whereas u-shaped profile was observed for solid-air stream.

It can be seen from table 3.3 that maximum researchers used CFD code FLUENT to predict the erosion wear of the slurry pipe line. Many of them implemented Euler-Lagrange (DPM) model with standard k-ϵ turbulence modeling scheme to solve the flow problem. The obtained results of DPM erosion model was giving approximate results of the real erosion problem.

After reviewing previous studies, the CFD code FLUENT 15.0 was found to be optimum for simulating the erosion wear in the present work. In this work, DPM model with the standard k-ϵ turbulence modeling along with the mixture property was applied to solve the multiphase flow through the pipe line. The particle type was set to inert in the injection setup of FLUENT. The solution was considered to be converged only when all the residuals fall below 10^{-5}.

3.10 Description of Computational Simulation

The simulation setup is performed in commercial CFD code FLUENT 15.0. To validate the model, previous published findings of Safae et al. (2014) and Zhang et al. (2014) was considered. The bottom ash is considered as solid particle having a density of 2200 kg/m^3 and mean diameter of 150 µm at 10% concentration. In the present work investigations are performed to analyse the influence pipe diameter, bending angle, flow velocity and bending radius ratio.

3.11 Piping Material and Attributes

A mild steel pipe bend is considered for the analysis of erosion wear in this study. The length of the pipe bend is 1.5 m and is sufficient enough to maintain fully developed flow. The geometry of the pipe was constructed in Creo. Figure 3.5 shows the detailed view of the flow domain.

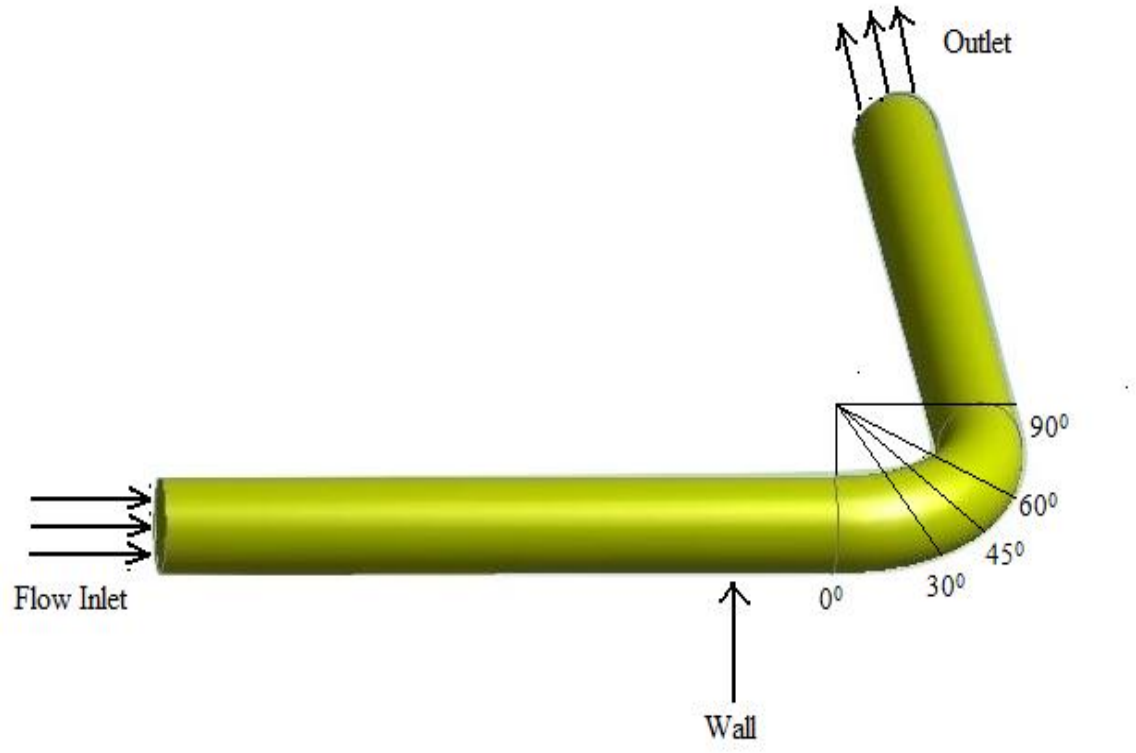

Figure 3.5: Horizontal pipe bend

3.12 Discretization of the Domain

In order to evaluate the flow behaviour accurately at every section of the pipe, the pipe was discretized into smaller number of elements. In ANSYS there are various meshing methods and mesh shape available such as tetrahedral, quadrilateral, hexahedral and triangular.

In the present work, the domain was divided into 247,754 hexahedral cells. Five Layers inflation with 1.2 growing rate is applied to precisely observe the boundary layer phenomenon. Figure 3.6 shows the meshed view of domain.

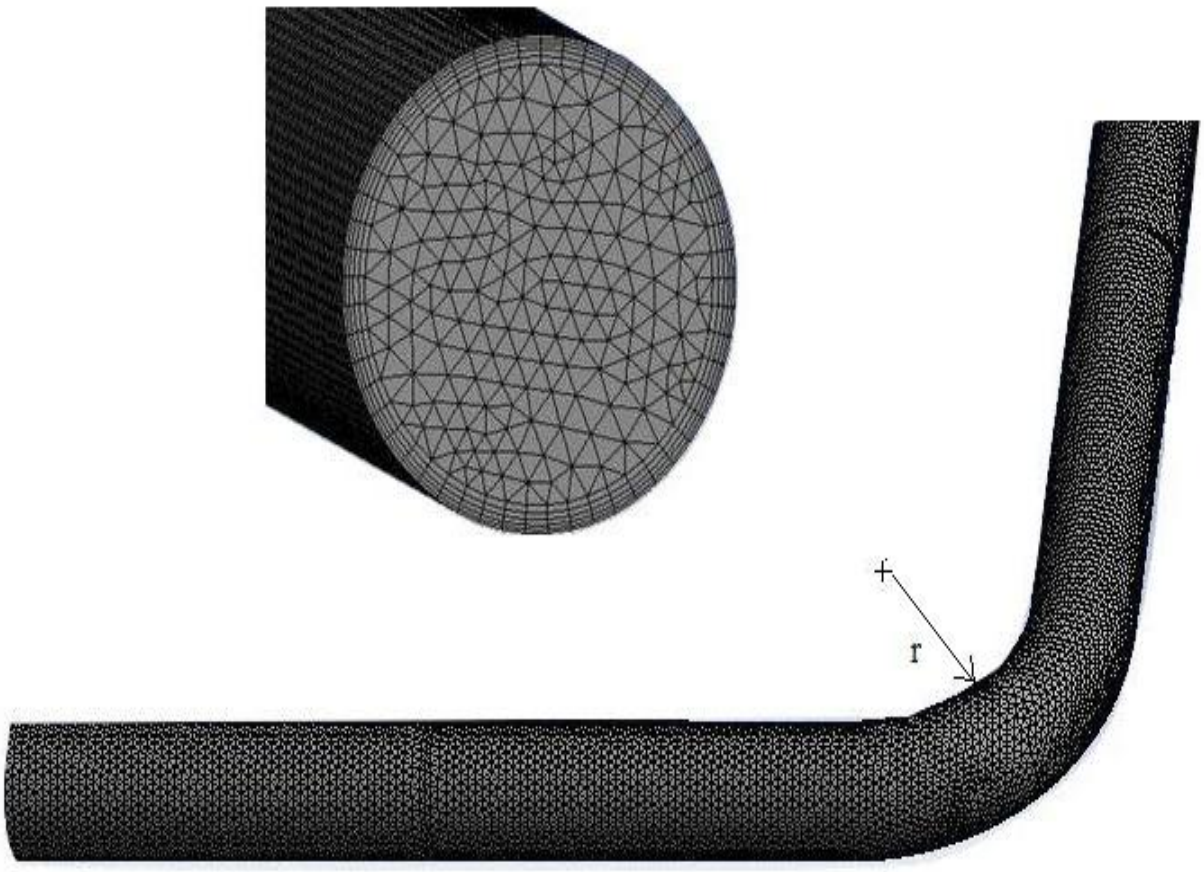

Figure 3.6: Pipe cross section with meshing

3.13 Description of Boundary Condition and Parameters

Referring to Figure 3.5, which shows the computational domain has three boundaries namely Inlet, Outlet and Wall. The domain has a single velocity inlet to allow the slurry flow, a single pressure outlet which was subjected to atmospheric pressure of 1 bar. The velocity of slurry was initially 2 m/s which were changed from 2 m/s to 8 m/s for further simulations. The turbulent intensity at inlet was 'medium' i.e. 5%. Wall surfaces were given standard boundary condition and simulation is carried out by considering rough wall having height of roughness as 2 μm. The discrete phase was Inert particles with reflect boundary conditions at wall. The impact angle was set to piece wise linear at the bend curvature.

Table 3.5: Boundary conditions and input parameters

Type	Description	Input
Model	Turbulence Scheme	• Standard K-ϵ
	Discrete Phase Modeling	• Near wall treatment : Standard wall function • Enable interaction with continuous phase • Physical model : Erosion/Accretion
Material	Description	• Flowing fluid (Water) • Solid Domain • Solid phase (Bottom Ash)
Injection Type	Release from surface : Inlet	• Velocity • Particle Size • Total Flow Rate • Stochastic Tracking : Discrete Random Walk
Operating Conditions	Gravitational acceleration Pressure	• -9.81 in vertical downward • 101325 Pa
Boundary Conditions	Inlet	• Velocity Inlet
	Outlet	• Pressure Outflow
	Wall	• Stationary • No slip • Roughness constant : 0.5 • Erosion model impact angle function : Polynomial • Velocity exponent : Constant
Convergence criteria		• 10^{-5}
Solution Controls	Discretization	• Pressure : Standard • Momentum : First order upwind • Turbulence kinetic energy: First order upwind
Solution initialization	Standard initialization	• Compute from all zones

The simulation was performed in CFD code FLUENT 15.0 using Discrete Phase Modeling (DPM) and standard k-ϵ turbulence modeling scheme, in order to find out the influence of particle size, bend orientation, pipe diameter, bending radius and flow velocity on the erosion wear of the pipe.

3.14 Solid-Liquid Properties

In this study the investigation of erosion wear caused by the flow of Solid-Liquid multiphase was carried out. The multiphase slurry of water and bottom ash was simulated in this work. The detail of Solid and Liquid phase properties are discussed in Table 3.6.

Table 3.6: Property of Multiphase flow

Flowing Fluid	Water
Density (kg m^{-3})	1000
Solid	Bottom Ash
Density (kg m^{-3})	2200
Particle Size (μm)	150
Particle Shape	Spherical
Velocity	2 to 8 m/s

CHAPTER 4

RESULTS AND DISCUSSIONS

Erosion wear is a complex phenomenon to understand as it depends on several operating parameters. Pipe bends are the vital component of most of industrial pipelines configurations. In this work simulation investigation is performed to study erosion wear caused by bottom ash-water slurry of mild steel pipe bend by using CFD code FLUENT 15.0. Bottom ash and water slurry is simulated at different flow velocity ranging from 2 to 8 m/s and at low solid concentration of 10%. An attempt is made to observe the influence of bending angle, pipe line diameter, bending radius to pipe diameter (r/D) ratio and flow velocity on the erosion wear characteristics. The results are plotted graphically however several contours and distributions are obtained at various operating conditions. The obtained results are compared with the previous published findings and are found to be in agreement with them.

4.1 Model Validation

The simulations results obtained from the present study are validated with the previous published work of Safae et al.

Safae et al. 2014 investigated the influence of particle size on the erosion wear of a 90^0 pipe bend. They reported a simulation study of erosion wear by using CFD code FLUENT and DPM model. The work was performed on a 0.016 m long aluminium elbow of 0.0032 m diameter. Copper particle was used as erodent with size range from 10 nm to 100 μm and the continuous phase was water with flow velocity in range of 5-20 m/s. Their result showed that the maximum erosion rate caused by 10, 50 and 100 μm particles at 2% volume fraction and 10 m/s velocity are as 3×10^{-5}, 4.2×10^{-5} and $5 \times 10^{-5} kg/m^3$ respectively.

At same operating conditions and flow domain, the maximum erosion rate predicted by present study for 10, 50 and 100 μm copper particles are as 3.2×10^{-5}, 4.36×10^{-5} and $5.23 \times 10^{-5} kg/m^3$ respectively. Figure 4.1 and figure 4.2 shows the agreement between the previous work of Safae et al and present study. On comparison with the previous study it was found that the present work predicts results with an error of approximately 10-12%.

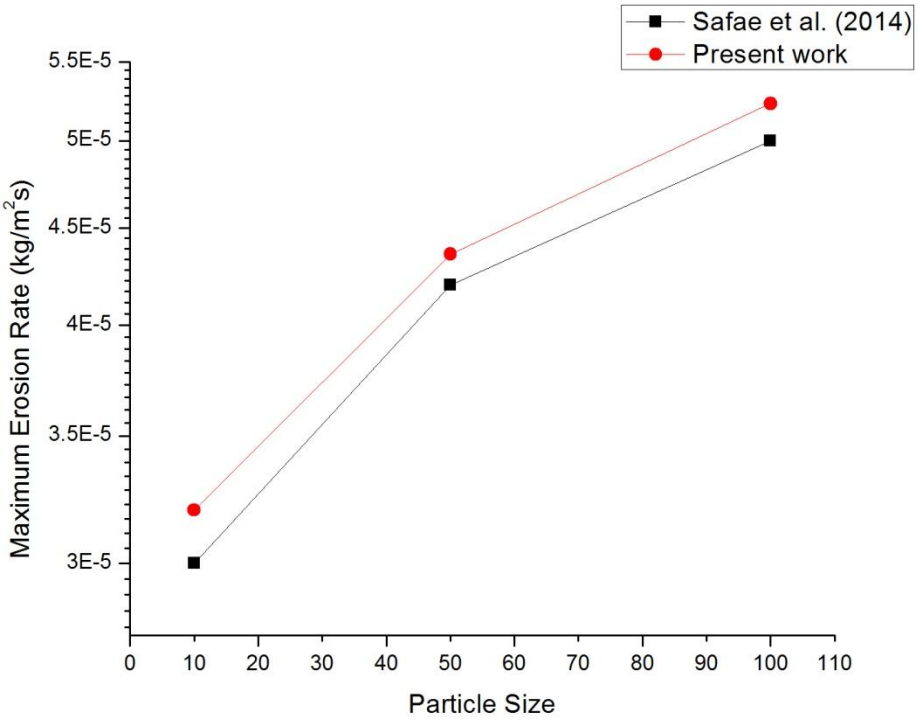

Figure 4.1: Comparison of present work with Safae et al. 2014

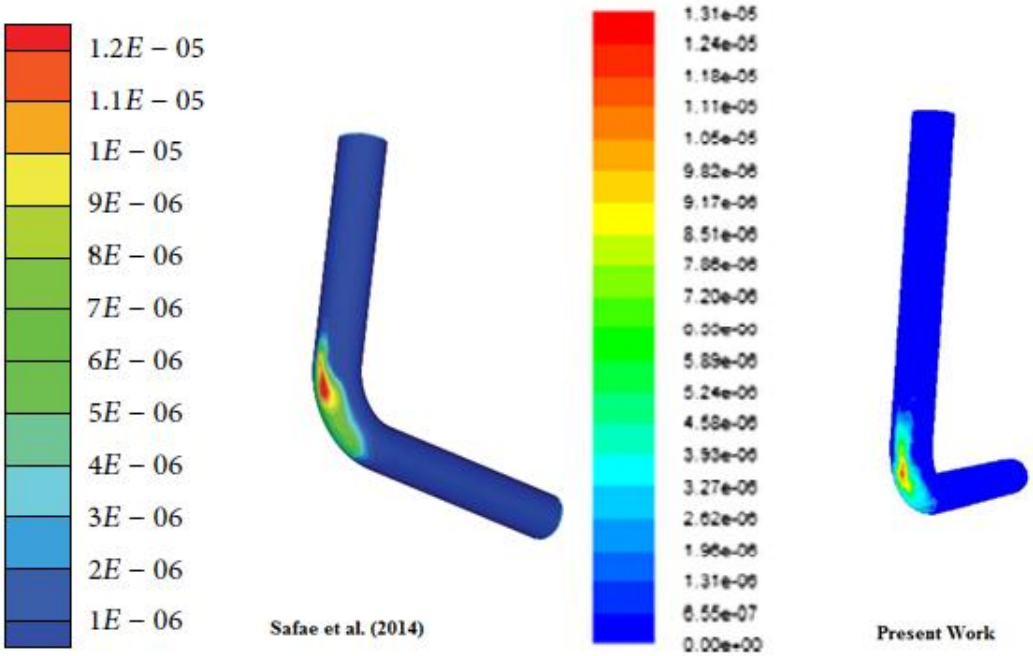

Figure 4.2: Erosion contours of Safae et al (2014) and Present work

4.2 Range of Parameters

Erosion behaviour is analysed at different conditions of operating parameters, several tests are performed as summarised in table 4.1. Tests 1 to 3 are performed to study the influence of bending angle on the erosion wear characteristics of slurry pipe line. Test 4 and 5 is accomplished to account the effect of pipe line diameter and flow velocity while Tests 6 to 8 is carried out to analyse the bending ratio effect on erosion rate.

Table 4.1: Test conditions and parameters

Test	**Velocity (ms^{-1})**	**Particle size (μm)**	**Concentration (%)**	**Bend Angle**	**Radius Ratio (r/D)**	**Pipe Diameter (mm)**
1	2 & 8	150	10	45^0	1.5	50
2	2 & 8	150	10	60^0	1.5	50
3	2 & 8	150	10	90^0	1.5	50
4	2 & 8	150	10	90^0	1.5	50 to 250
5	2 to 8	150	10	90^0	1.5	150 & 250
6	2 & 8	150	10	90^0	1.5	50
7	2 & 8	150	10	90^0	2	50
8	2 & 8	150	10	90^0	2.5	50

4.3 Effect of Bend Angle on Erosion Wear in Pipe Line

Investigation of erosion wear is carried out for straight pipe and pipe bends having different bending angle of 45, 60 and 90^0 to analyse the bending angle effect on erosion wear characteristics. The simulation study is performed by applying operating conditions from test 1 to 3 as listed in table 4.1. The influence of bending angle on maximum erosion rate is represented in figure 4.3. Highest erosion wear is observed for the 90^0 bend. The lowest magnitude of erosion rate is observed for straight pipe as 1.47×10^{-6} which gets increased to $4.11 \times 10^{-6}\ kg/m^2$.s for 90^0 bend at 8 m/s velocity. It is noticed that at the same operating conditions the erosion rate increases as the bending angle increases from 30 to 90^0. Total three times increment in erosion rate is observed when the geometry changes from straight pipe to 90^0 bend. As per the geometrical construction of these bends the particle

impact angle is higher for 90^0 bend on comparison with other bends. The high impact angle will increase the value of impact angle function f(α) in Eq. 3.9 as f(α) directly affects erosion rate thus the larger angled bend is found to be more eroded. Moreover the particles undergo numerous collisions with the inner wall region because higher angled bend has relatively larger length than the small angled bend. For larger angled bend the region of maximum velocity is noticed near the bend curvature area thus more damage is noticed at curvature while for lower angled bend maximum velocity is distributed uniformly. It is also found that as the bend angle is reducing from 90 to 45^0, the strength of the secondary flow also diminishes along with it. At the curvature region of 90^0 bend, the flow turbulence along with the secondary flow enhances to a great extent, this will increase circumferential movement of particles and leads to more collision with the wall. Thus it can be advantageous to swap larger angled bend of with smaller angled bend. The obtained results are in well agreement with the findings of Chen et al. 2015.

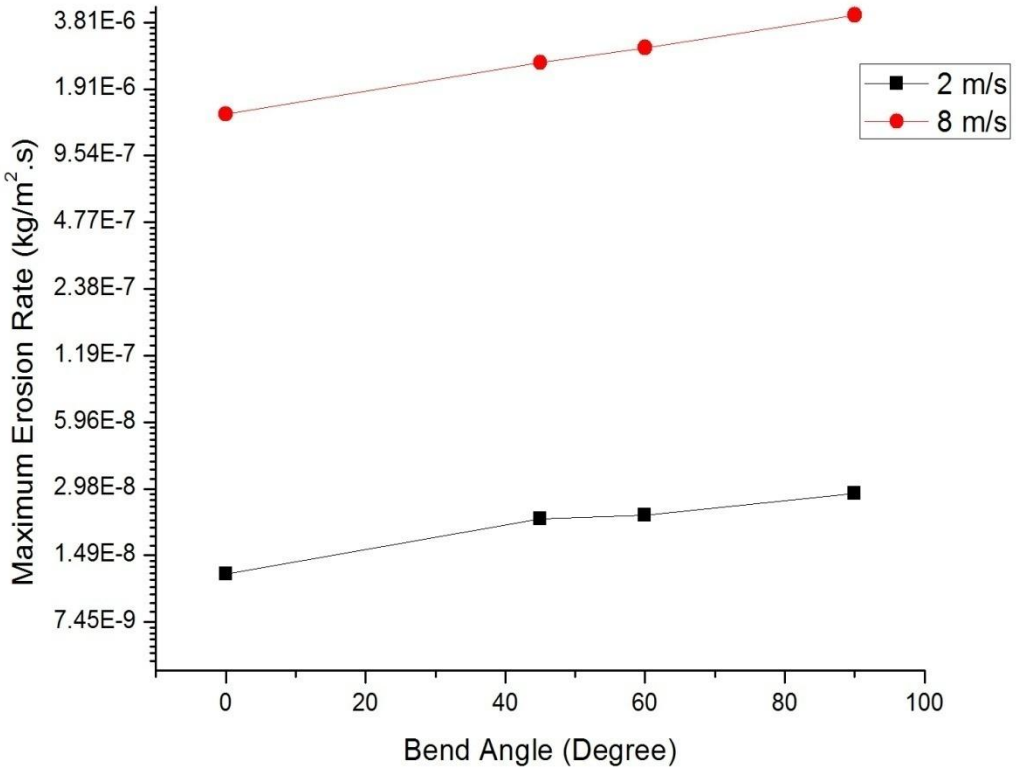

Figure 4.3: Influence of bending angle on maximum erosion rate

4.3.1 Contours of Erosion Rate

Figure 4.4 and 4.5 shows the erosion wear contours for straight pipe, 45, 60 and 90^0 bends at 2 and 8 m/s velocity. The red colour demonstrates high erosion while the blue signifies least erosion. It can be observed from the figure that intense erosion is found at higher velocity while it is negligible at low velocity. The maximum erosion damage is observed for 90^0 bend amongst the other bends. It can be observed from the contours that in pipe bends less erosion is observed near the entrance region while it grows up to the inlet of bend curvature and reaches to maximum at curvature whereas for straight pipe the erosion is highly located near the centre to exit region of pipe wall. The secondary flow is found to be more intense for 90^0 pipe causing more collision of ash particles and pipe wall. The position of maximum erosion is also investigated at different velocities. The location of maximum erosion caused by low velocity of 2 m/s is found around 45 to 65^0 of bend curvature while it is located at 30 to 65^0 for high velocity of 8 m/s.

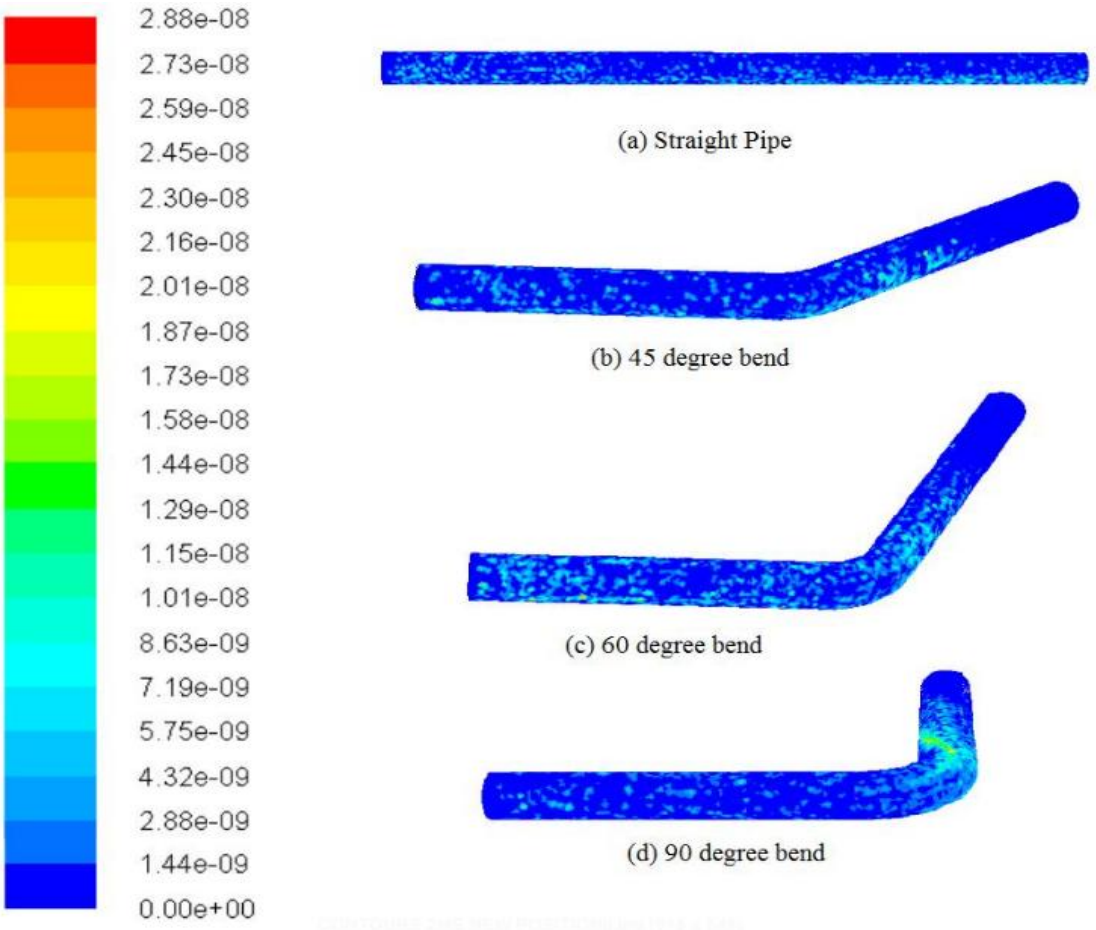

Figure 4.4: Contours of erosion at pipe wall for 2 m/s velocity

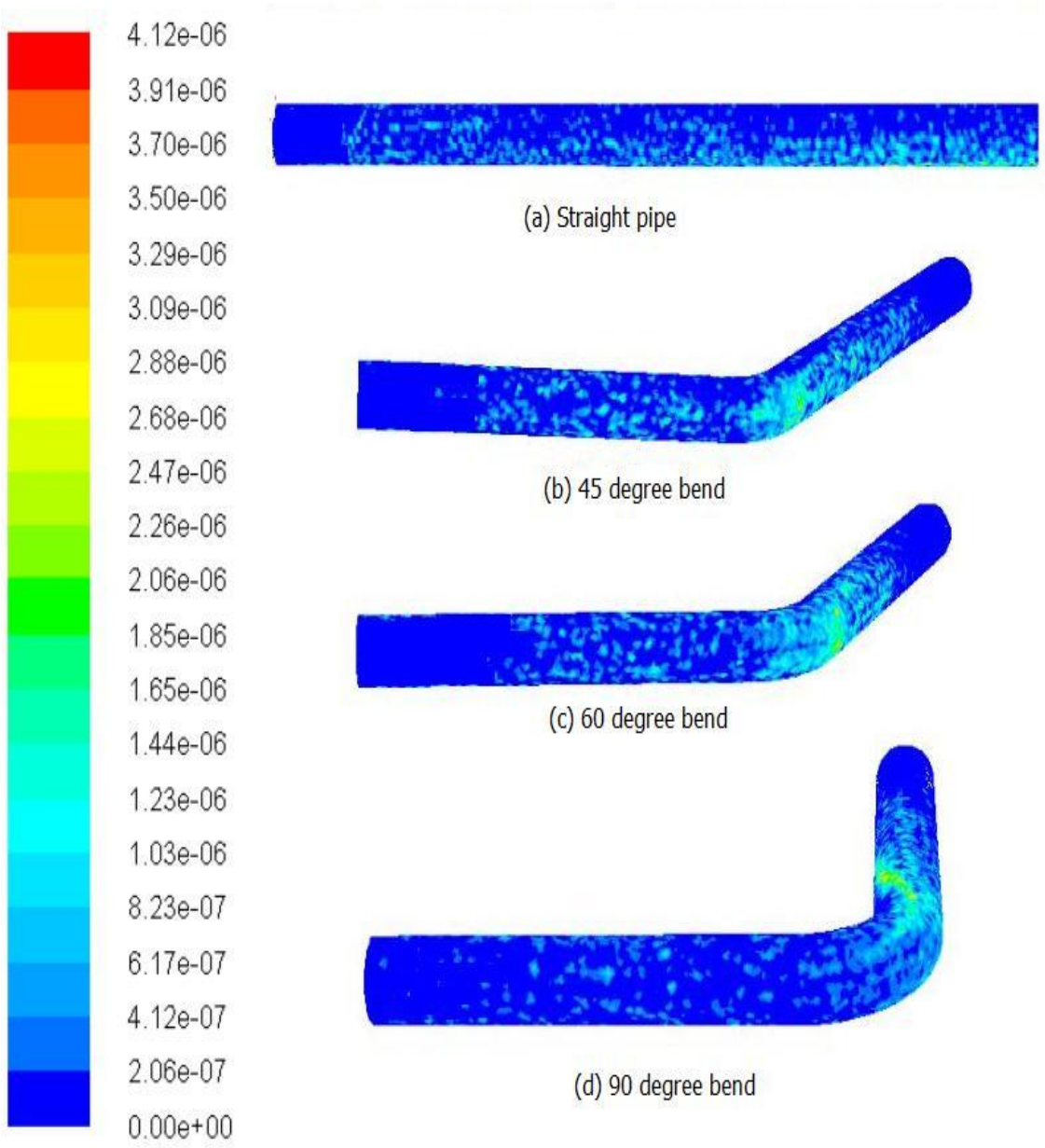

Figure 4.5: Contours of erosion at pipe wall for 8 m/s velocity

The path lines of particles through a 90^0 pipe bend at 2 m/s velocity is represented in figure 4.6. It can be observed that the particle follows parallel path before entering in the curvature region while as the particles entered in the bend area they will travel through a narrow region and gets deviated from the parallel regimes. These deviated particles approach towards the wall and collide with it violently.

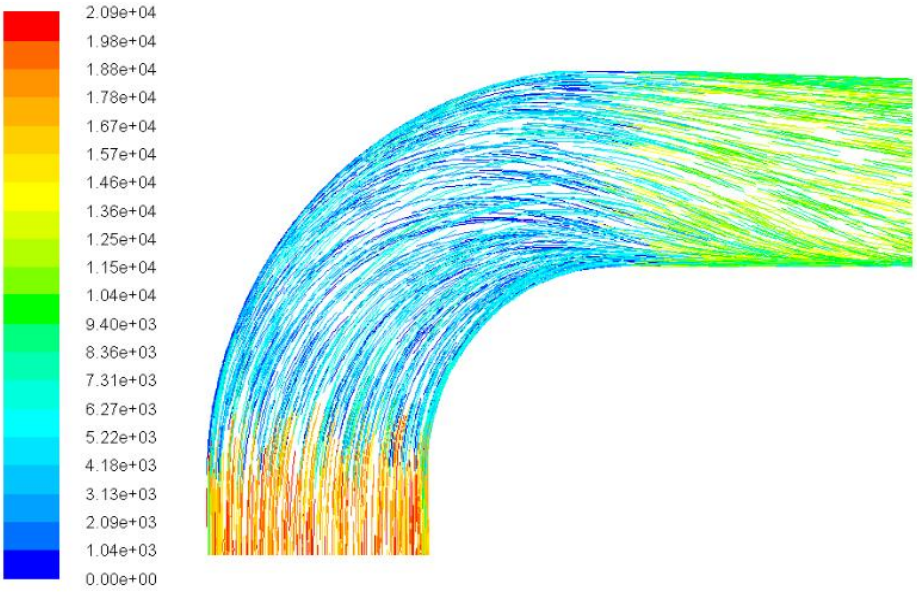

Figure 4.6: Top view of 90^0 bend representing path lines of particles

The non-uniform structure of bend influence the flow and causes un even distribution of velocity and pressure. Figure 4.7 shows pressure and velocity distributions at different curvature sections of a 90^0 pipe bend. The noticeable observations from this distribution is that velocity is found to be maximum at inner wall 60^0 section of the bend curvature while maximum pressure is observed at the outer wall of bend curvature near 45 to 60^0.

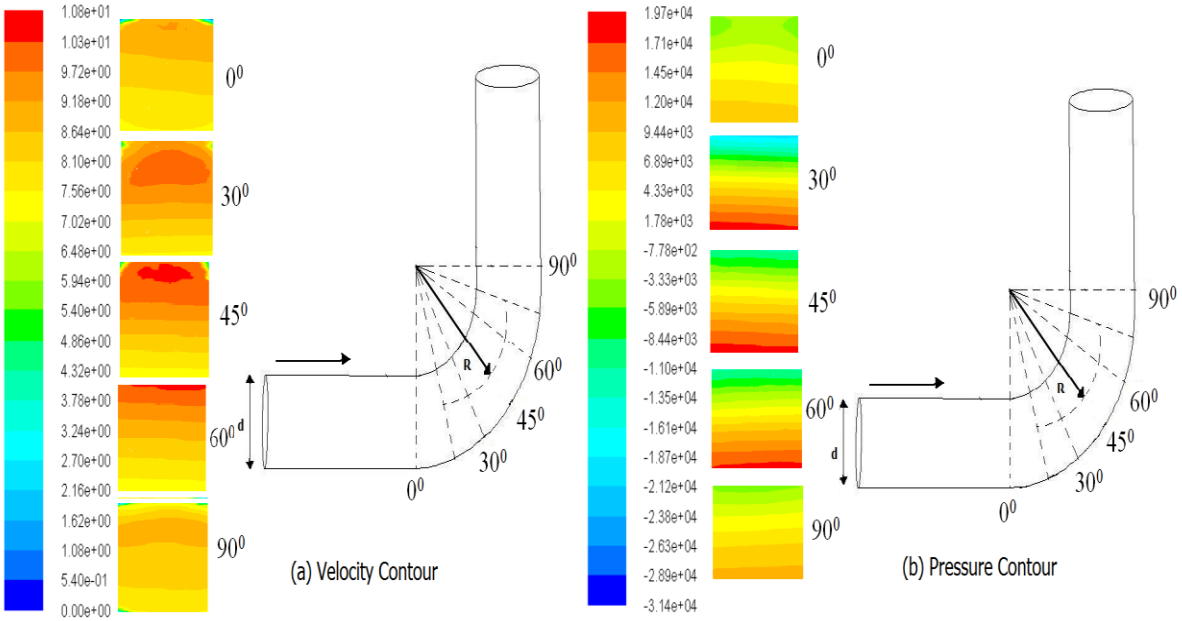

Figure 4.7: Velocity and pressure contours at different curvature sections of 90^0 pipe bend

4.4 Influence of Pipe Diameter on Erosion Wear in Pipe Line

The influence of pipe diameter on erosion wear behaviour is shown in figure 4.8. For this investigation different pipe bends are considered having diameter variation from 50 to 250 mm. The slurry having 10% solid concentration is allow to flow at two different velocity of 2 and 8 m/s. The results show inverse relationship of erosion rate and pipe diameter. A sharp decrement in the erosion wear is observed with the increase in diameter of pipe. It is found that the magnitude of maximum erosion rate was reduced by more than 11 times from 3.913×10^{-8} to 3.305×10^{-9} $\frac{kg}{m^3}$.s when the pipe diameter is changes from 50 to 250 mm at velocity of 2 m/s. The decrement in erosion rate is found as 27.5, 64.7, 55.9 and 25.2% when the pipe diameter increases from 50 to 100, 100 to 150, 150 to 200 and 200 to 250 mm respectively at 2 m/s velocity as shown in figure 4.8. It can also noticed from the figure 4.9 that further enlargement in pipe diameter beyond 200 mm will causes less reduction in erosion rate and the decreasing trend tends to be stabilized. The reason for such behaviour is that for smaller diameter pipes the boundary layer is comparatively thin and thus particle enters in the wall region with more ease. The turbulence for a shorter diameter pipe is more intense that helps the particles to gain extra momentum and hit the wall with great impact results in severe erosion. The results are in agreement with the study of Zeng et al. 2013 and Peng et al. 2016.

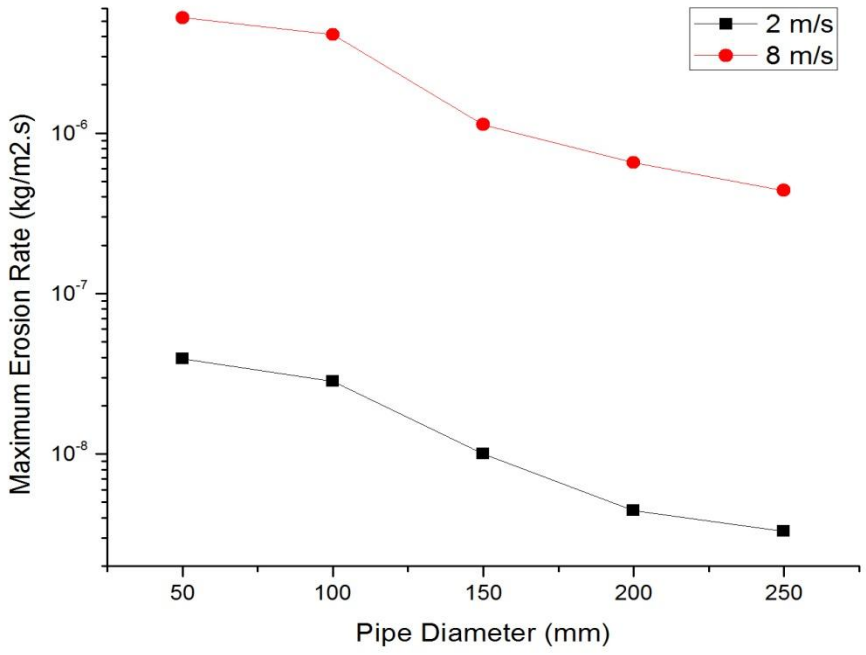

Figure 4.8: Effect of pipe diameter on maximum erosion rate

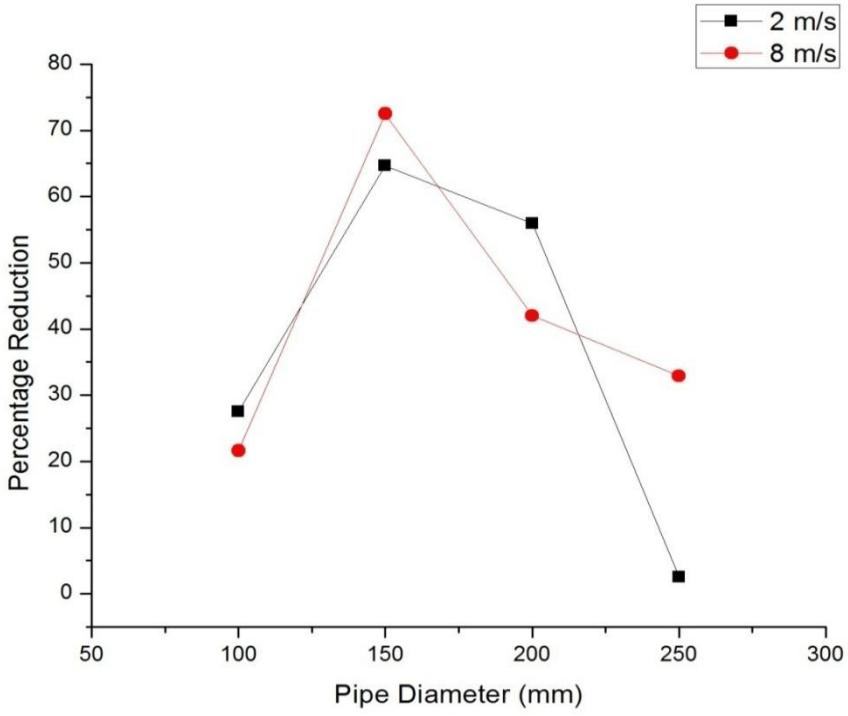

Figure 4.9: Percentage reduction in erosion rate with pipe diameter

4.4.1 Contours of Turbulent Intensity

The flow turbulence is characterized by turbulence intensity and is expressed in percentage. Figure 4.10 and 4.11 represents the turbulent intensity at the bend outlet of various diameter pipe lines for 2 and 8 m/s velocity. In the contours the red area represents highly turbulent flow while blue area meant to be lesser turbulent flow. It can be depicted from the contours that the low diameter pipes (50-150 mm) have more turbulence zone near the pipe wall boundary thus more erosion is observed in that region while the flow is found to be stable near the centre line of the wall. For higher diameter pipes (200-250 mm), the turbulence intensity was found to be stronger near the pipe line centre and becomes less across the wall which results in lesser erosion for such pipes. In Large diameter pipes the maximum velocity region is less and flow is comparatively stable than the low diameter pipes at the same velocity. The highest turbulent region is noticed for 50 mm diameter pipe bend.

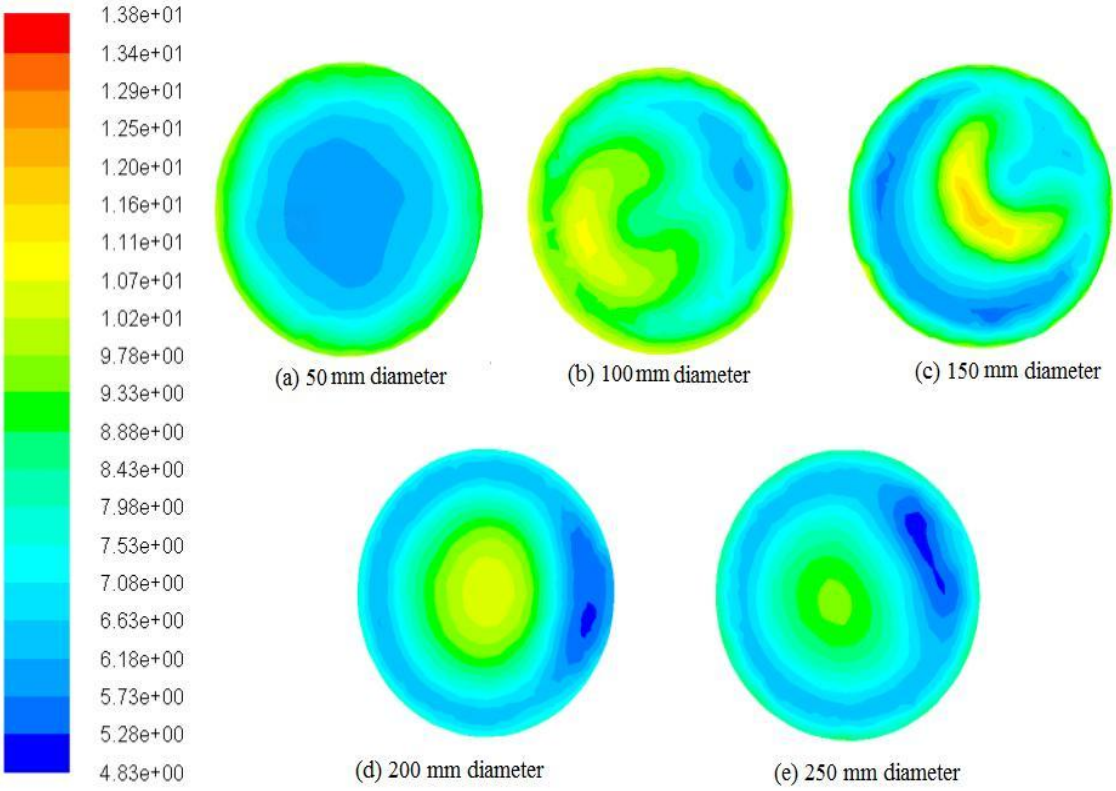

Figure 4.10: Turbulence intensity contours at the outlet of different diameter bends at 2 m/s

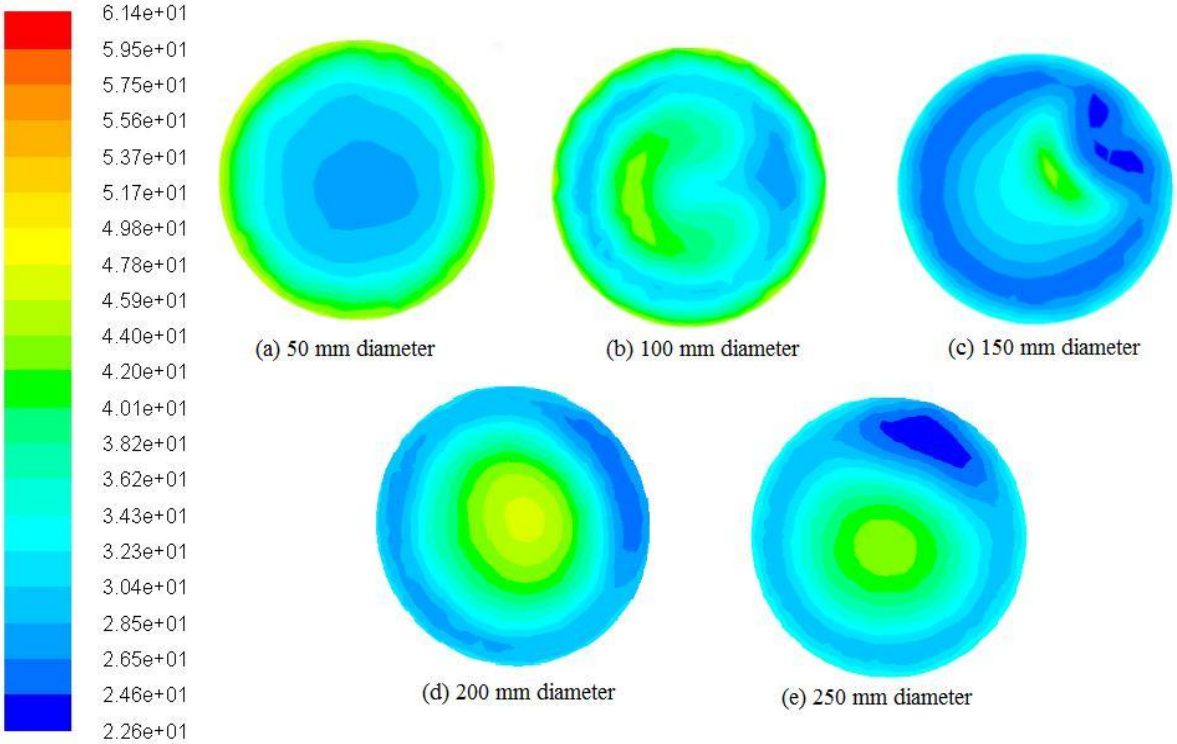

Figure 4.11: Turbulence intensity contours at the outlet of different diameter bends at 8 m/s

4.5 Effect of Flow Velocity on Erosion Wear in Pipe Line

The influence of flow velocity on the erosion wear characteristics are illustrated in figure 4.12. For this study slurry mixture having 10 % solid content by weight is allow to flow at different velocity ranging from 2 to 8 m/s through 150 and 250 mm diameter pipe bend. The operating conditions for this study are listed in test 4 in table 4.1. Figure 4.11 illustrates the variation occurred in the magnitude of erosion rate with the change in the flow velocity. A dependence of erosion rate on velocity is noticed and it is found be growing exponentially with the increase in velocity. It is observed that magnitude of maximum erosion rate for 150 mm diameter pipe line is increased to approximately 13 times when the flow velocity exceeds from 2 to 4 m/s also 3.8 and 2.2 times increment is noticed when velocity changes from 4 to 6 and 6 to 8 m/s respectively. The erosion wear of pipe line is found to be negligible at velocities lower than 2 m/s and grows exponentially at higher velocities. At higher velocity, the impact energy of the flow is also being high due to which the particles collides with wall with more force resulting in severe erosion.

For 250 mm diameter pipe the highest magnitude of erosion rate is found as $4.40 \times 10^{-07} kg/m^2 s$ at 8 m/s velocity while it is reduced to $3.31 \times 10^{-09}\ kg/m^2 s$ and becomes negligible when the velocity approaches to 2 m/s. The influence of velocity on erosion rate is found to be most significant amongst the other parameters. The obtained results are in agreement with the study of badr et al. 2003 and habib et al. 2007.

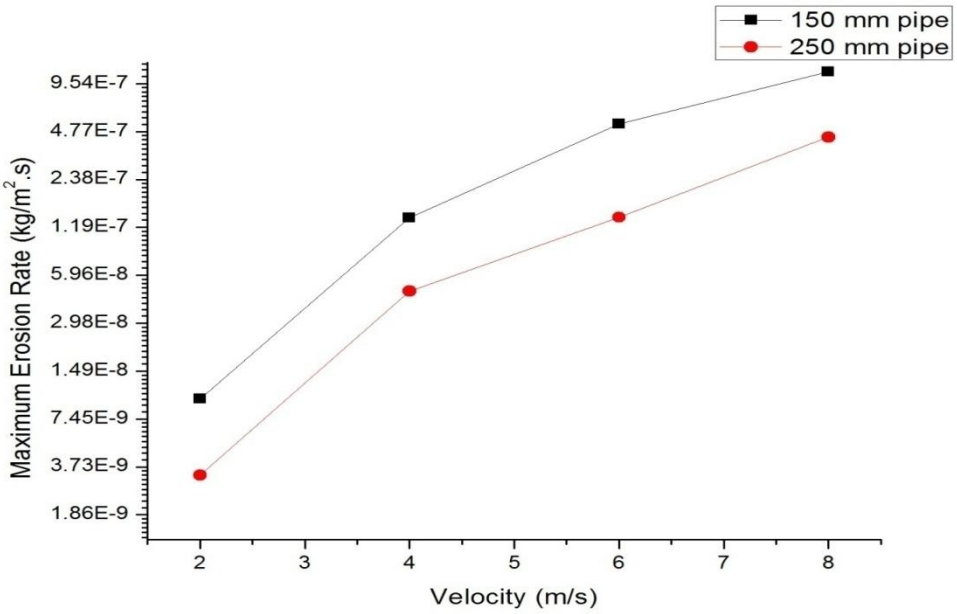

Figure 4.12: Erosion rate vs Velocity at two pipe diameters

4.5.1 Contours of Velocity Vectors

The direction and magnitude of velocity can be allocated with the help of velocity vectors. Figure 4.13 represents the velocity vector through 150 mm diameter pipe at 2 m/s, it can be noticed that flow velocity is higher near the inner wall of curvature of pipe. Erosion rate is found to be much high at the outer wall of the bend curvature rather than the inner wall as the particles gets deviated from the fluid stream due to their inertia. For the investigation of secondary flow the velocity vectors at different velocity of 2, 4, 6 and 8 m/s are represented at outlet of 150 and 250 mm pipe bends. Secondary flow is generated by counter rotating vortices due to the centrifugal effect. The velocity vectors at the outlet of 150 and 250 mm pipe bends are represented in figure 4.14 and 4.15, by observing the velocity vectors for both the pipes it is found that secondary flow intensity is more for 150 mm diameter pipe. Highly intense fully developed secondary flow is observed at 8 m/s velocity. Such flow contributes in pushing the solid particles towards the wall of pipe and is responsible for creating the particle-wall impact. It can be noticed from the vectors that at 8 m/s velocity huge recirculation developed in the flow at the outlet of both the pipe line.

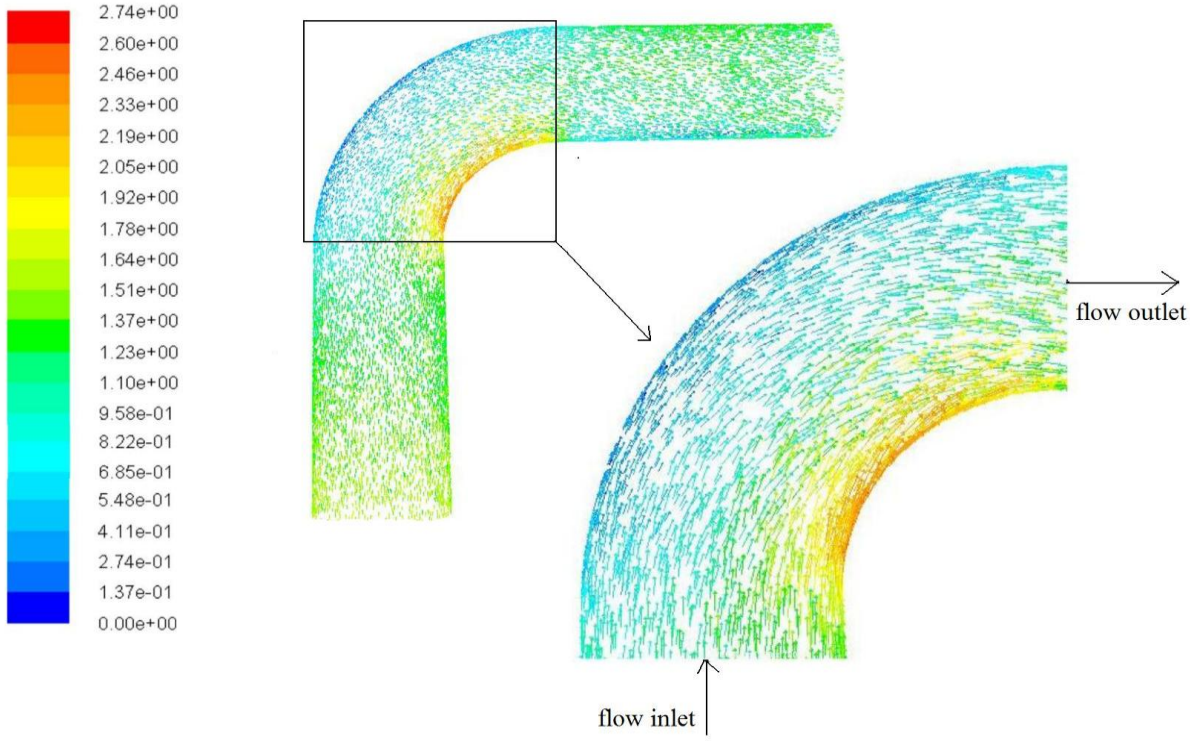

Figure 4.13: Velocity vector through 150 mm diameter bend at 2 m/s velocity

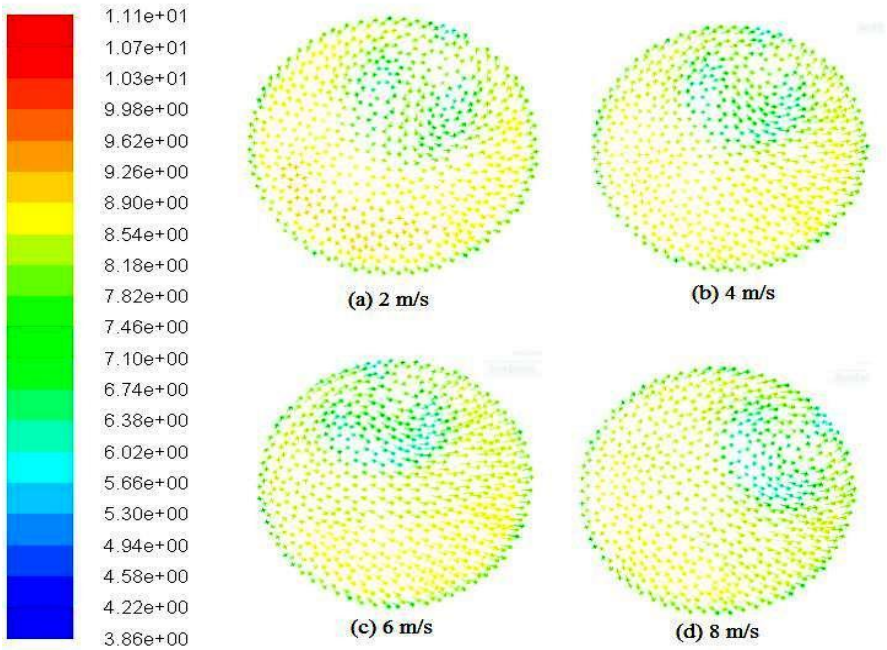

Figure 4.14: Velocity vector at outlet of 150 mm diameter pipe at different velocity

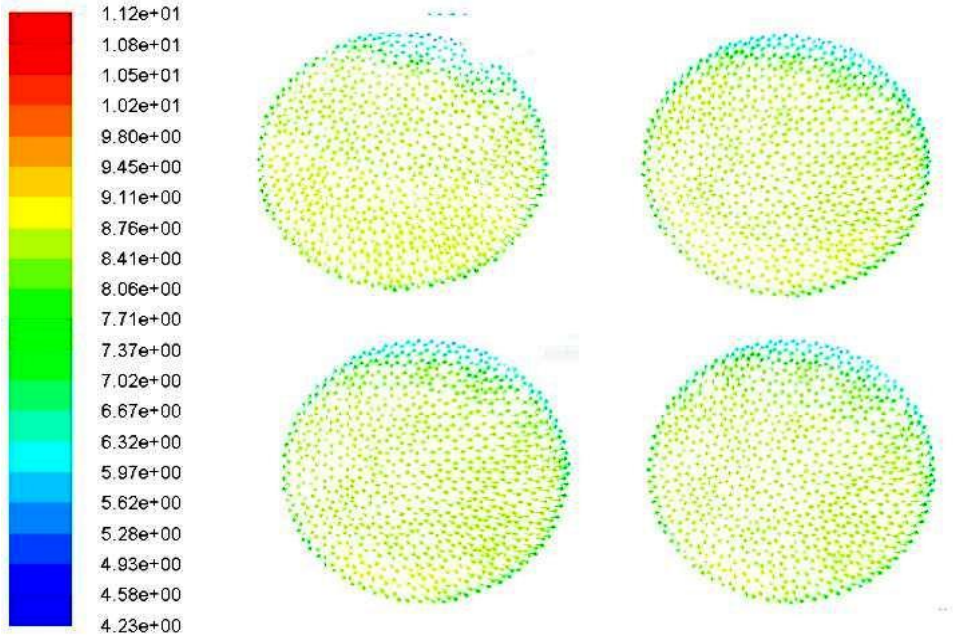

Figure 4.15: Velocity vector at outlet of 250 mm diameter pipe at different velocity

4.6 Effect of Bending Radius (r/D ratio) on Erosion Wear in Pipe Line

Influence of bending ratio on the maximum erosion wear rate is investigated by considering bends of radius ratio 1.5, 2 and 2.5 respectively. For this investigation the slurry mixture having 10% solid content is allow to flow through pipes having different bending ratio at 2

and 8 m/s velocity. The parametric conditions for this study are listed in test conditions 5 to 7 in table 4.1. Figure 4.16 illustrates the effect of pipe bending radius on the erosion rate of pipe line. The erosion rate was found to be gradually decreased when the r/D ratio increased from 1.5 to 2.5. As the diameter of the pipe is fixed to 100 mm for these tests, a greater value of r/D will makes the pipe line longer due to which the erodent will flow more steadily and causes less collision with the pipe wall. Reduction in erosion rate of approximately 66% and 18% at 2 m/s velocity is noticed when the bending ratio is increased from 1.5 to 2 and 2 to 2.5 respectively. For the higher r/D ratio the erodent requires less centrifugal force to travel and thus their wall hitting possibility is greatly reduced. It is also found the fluid flow in larger radius bend is seems to be more similar to the flow in straight pipe. Thus it can be advantageous to uses higher bending radius pipe in industrial system to reduce the erosion wear. The result outcomes are in good agreement with the results of chen et al. 2015.

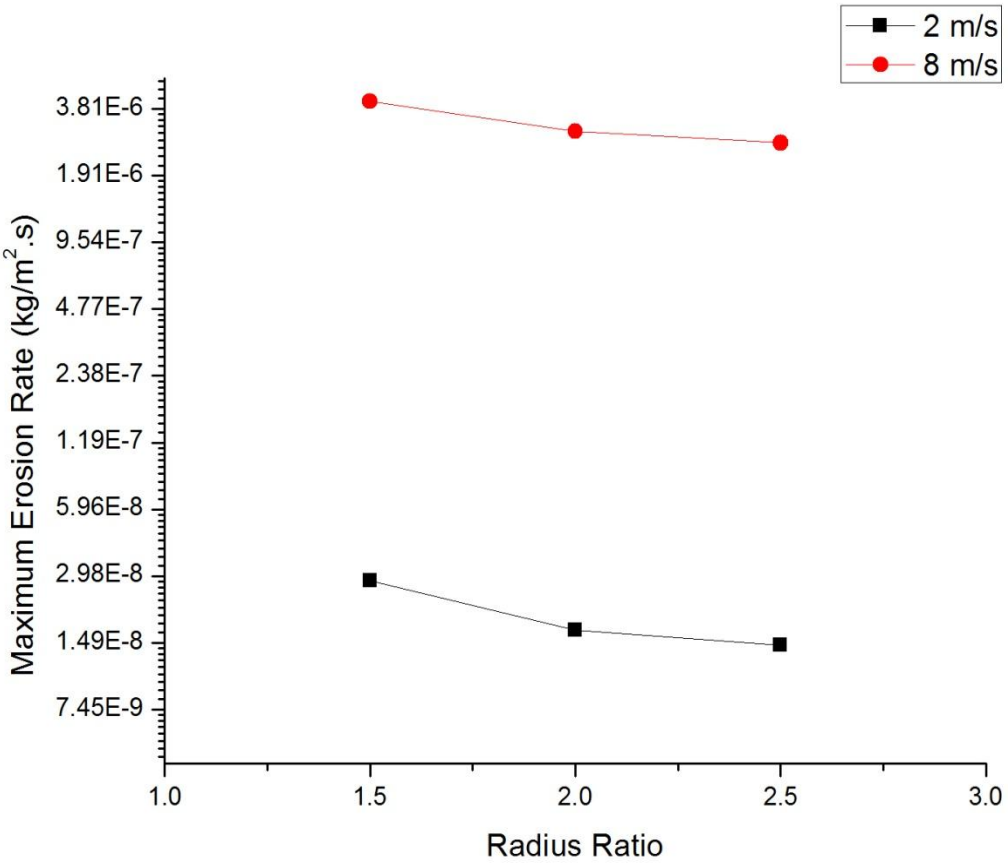

Figure 4.16: Effect of bending radius on maximum erosion rate

4.6.1 Contours of Velocity

Velocity plays a vital role in increasing the turbulence of the flow. The velocity magnitude of any flow is much influenced by the type of geometry. To analyse the velocity variation in different bending ratio pipes, the velocity contours is drawn at the outlet of pipe bends having radius ratio from 1.5 to 2.5 at 2 and 8 m/s velocity. It can be noted from the figure 4.17 and 4.18 that the maximum velocity region is found near the wall for low bending ratio pipes while this region gets shifted towards the central line of pipe and becomes less intense for higher bending ratio pipes. More circulation in flow is observed for the pipe with bending ratio of 1.5 as compared to other bends due to the influence of centrifugal force. The circulation magnitude mainly depends on magnitude of velocity and also on the type of geometry. It can be observed from the velocity contours that the flow circulation is higher for low bending ratio pipes due to which the particles are directed towards the pipe wall and creating collision with great impact thus results in more erosion. On the other hand low velocity shows less circulation and the flow field is observed to be smooth thus less erosion wear is noticed for such flows.

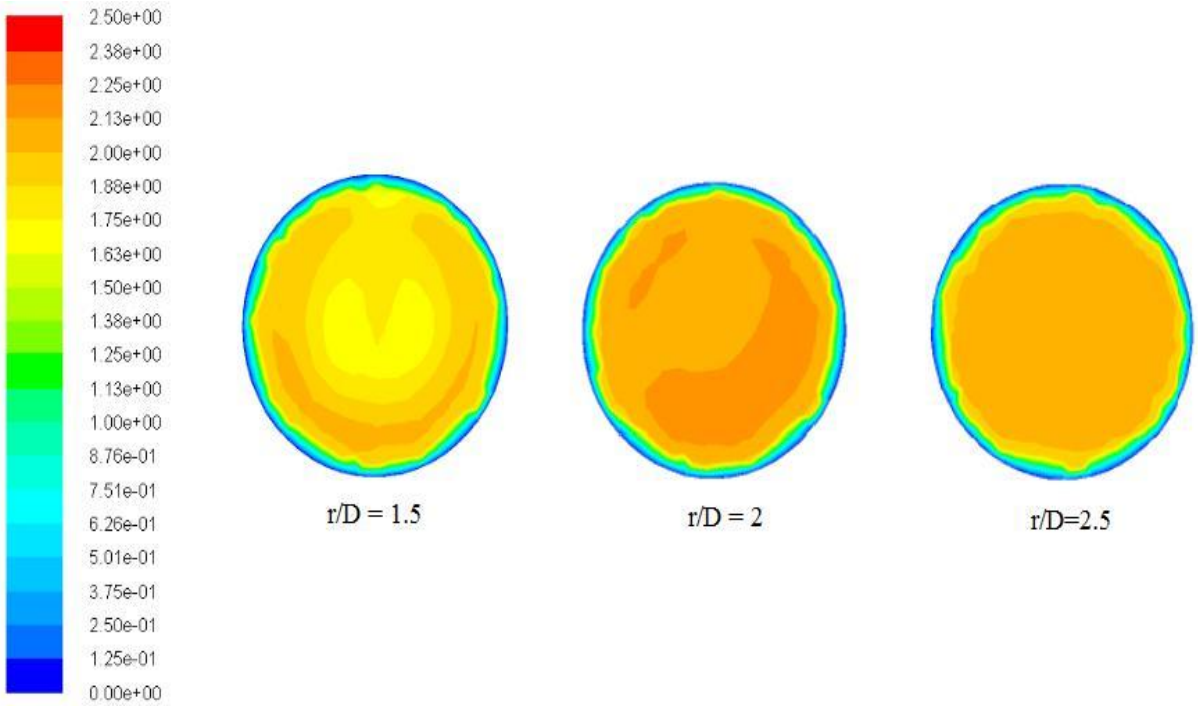

Figure 4.17: Contours of velocity at pipe outlet at 2 m/s

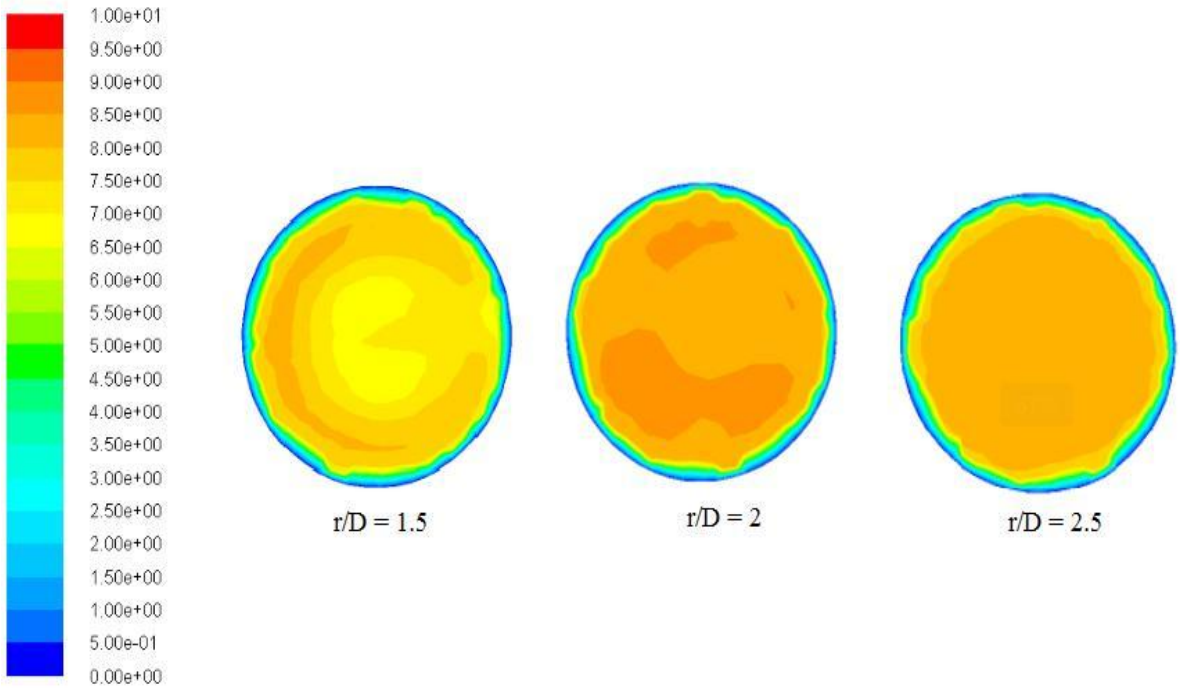

Figure 4.18: Contours of velocity at pipe outlet at 8 m/s

4.7 Velocity Distributions for Different Bending Radius Pipe Lines

The velocity of fluid or slurry mixture flowing through a pipe line is influenced by the pipe geometry. The velocity may increase or decrease from its initial value depending upon the shape of the fluid domain. To observe the flow velocity distributions at different geometry the distributions are plotted at the outlet of pipe bends with bending ratio (r/D) varying from 1.5 to 2.5 at velocities of 2 and 8 m/s and 10% concentration. The distribution of velocity at the pipe outlet is represented in figure 4.19 to 4.24. The results demonstrate the dependence of velocity with the flow domain configuration. It is noticed that the velocity distribution for lower bending ratio pipe (r/D ratio = 1.5) shows much variation in magnitude than the higher bending ratio pipes. This variation arises due to increase in the secondary flow. The larger bending ratio pipe lines shows comparatively less velocity variation as low flow turbulence is observed for such pipe lines. The maximum variation of velocity is found at the outer and inner wall of the bend outlet while it is found to be stable near the centre line.

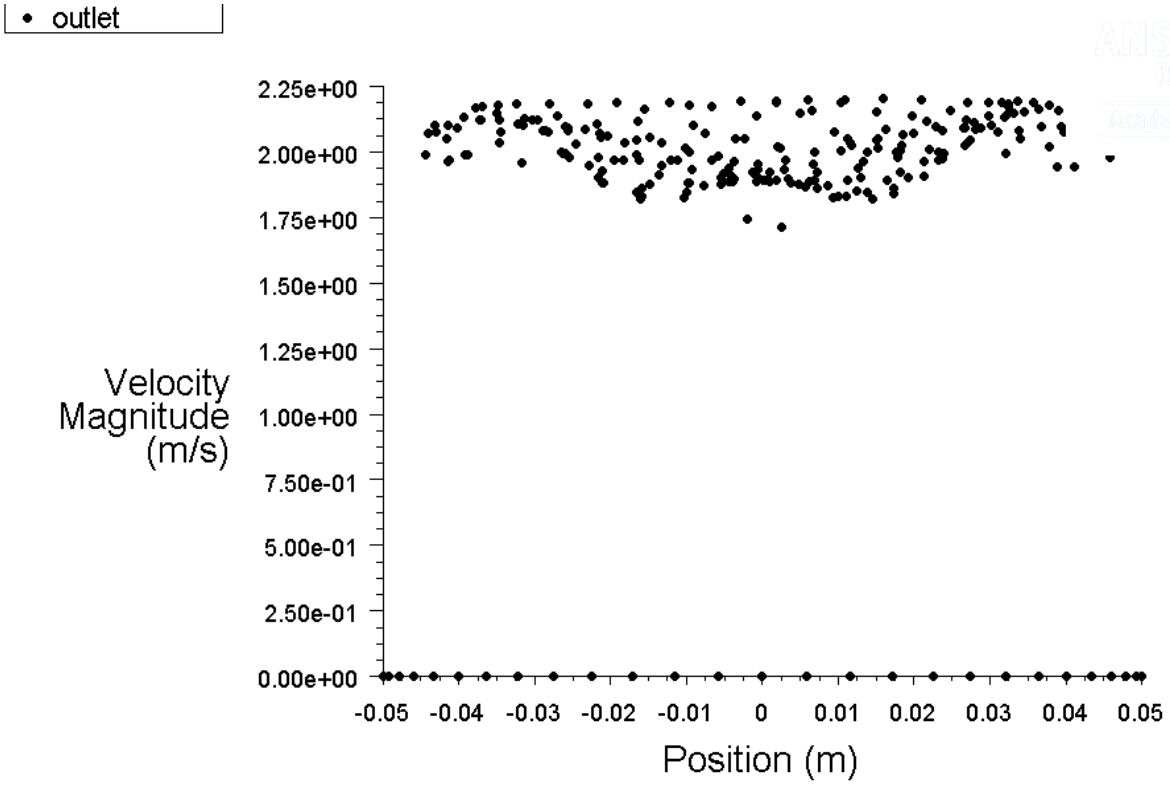

Figure 4.19: Velocity distributions at the bend outlet (r/D = 1.5) at 2 m/s

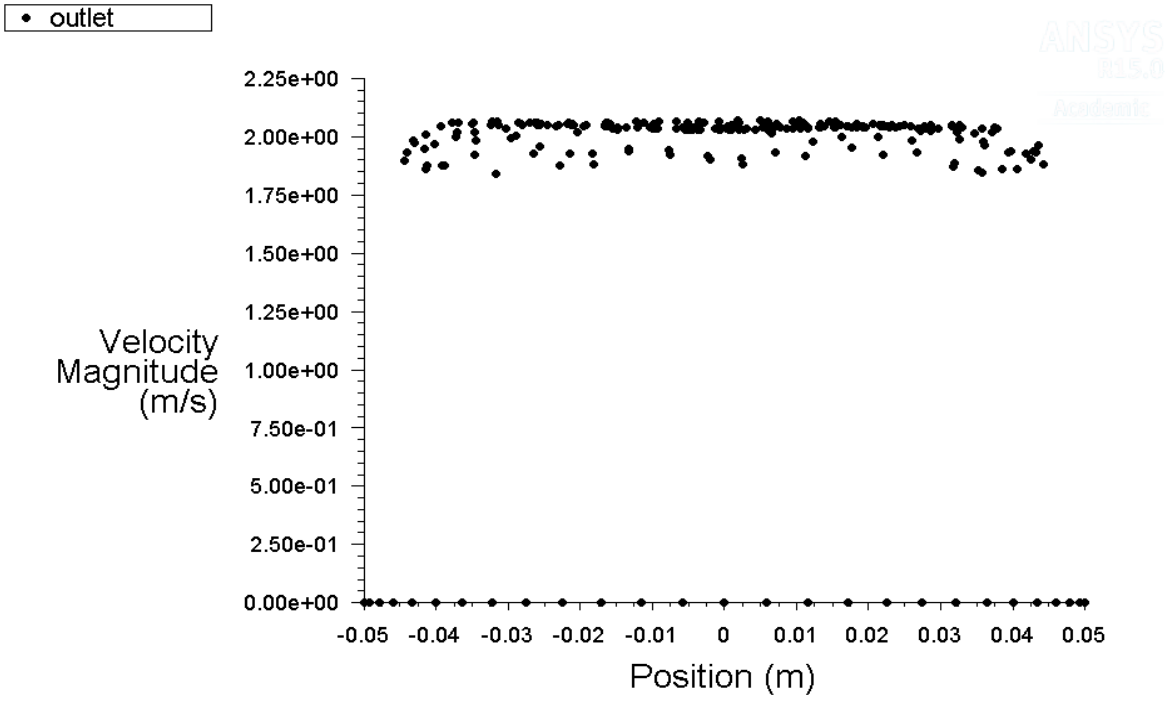

Figure 4.20: Velocity distributions at the bend outlet (r/D = 2) at 2 m/s

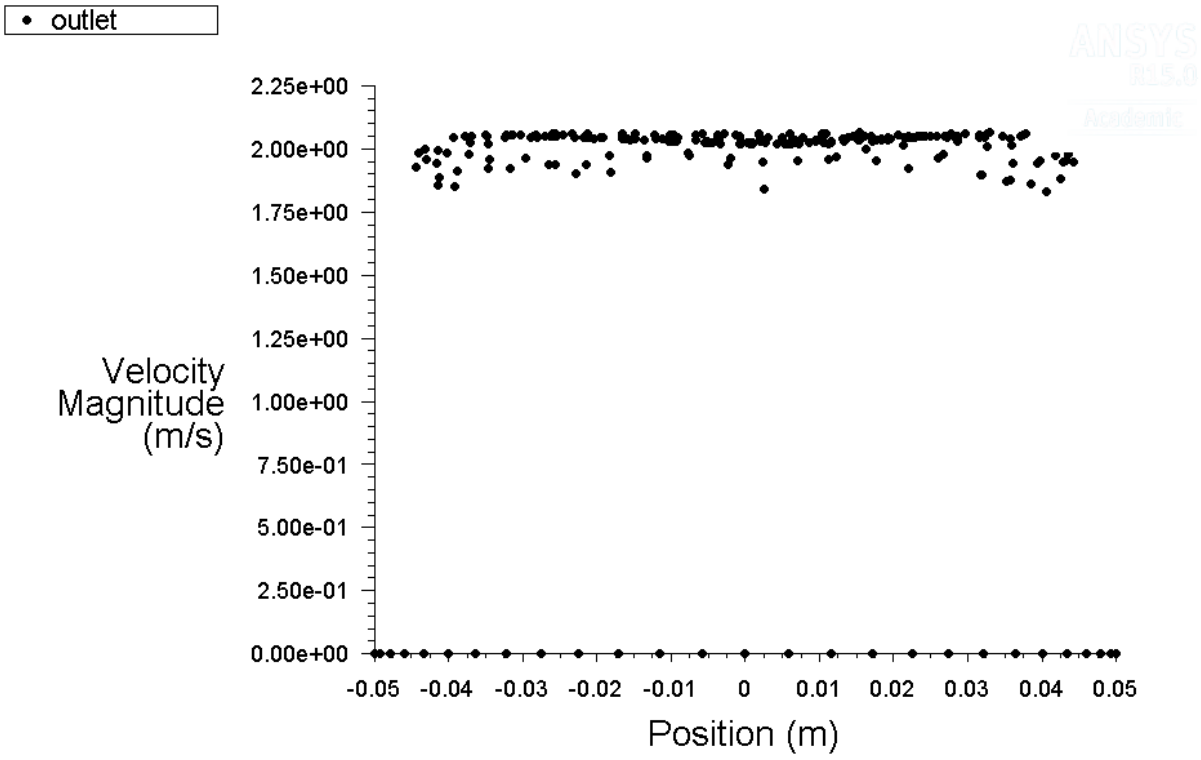

Figure 4.21: Velocity distributions at the bend outlet (r/D = 2.5) at 2 m/s

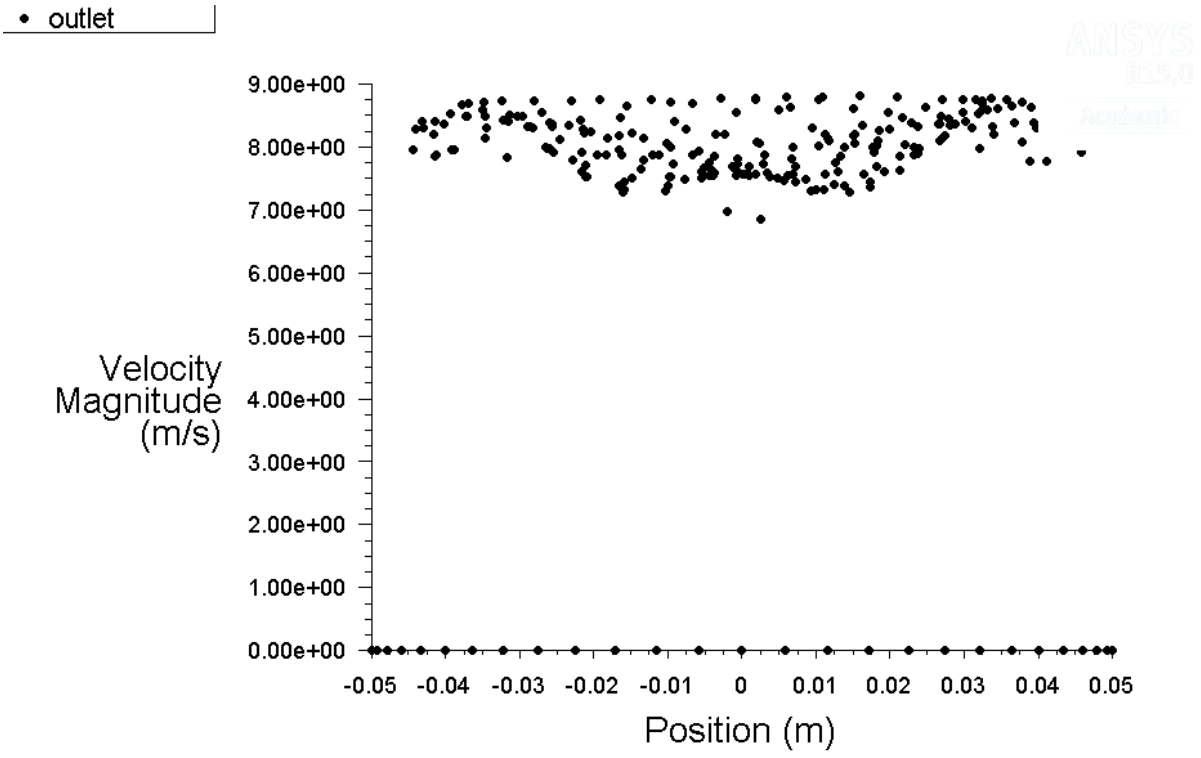

Figure 4.22: Velocity distributions at the bend outlet (r/D = 1.5) at 8 m/s

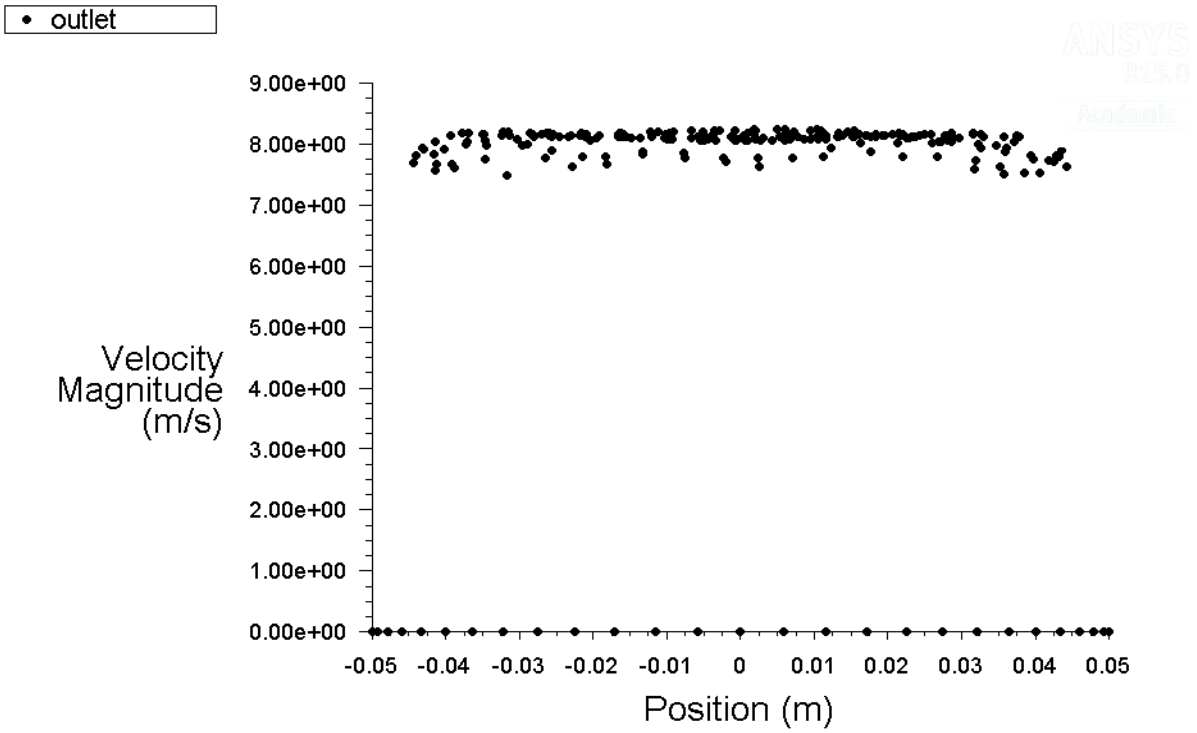

Figure 4.23: Velocity distributions at the bend outlet (r/D = 2) at 8 m/s

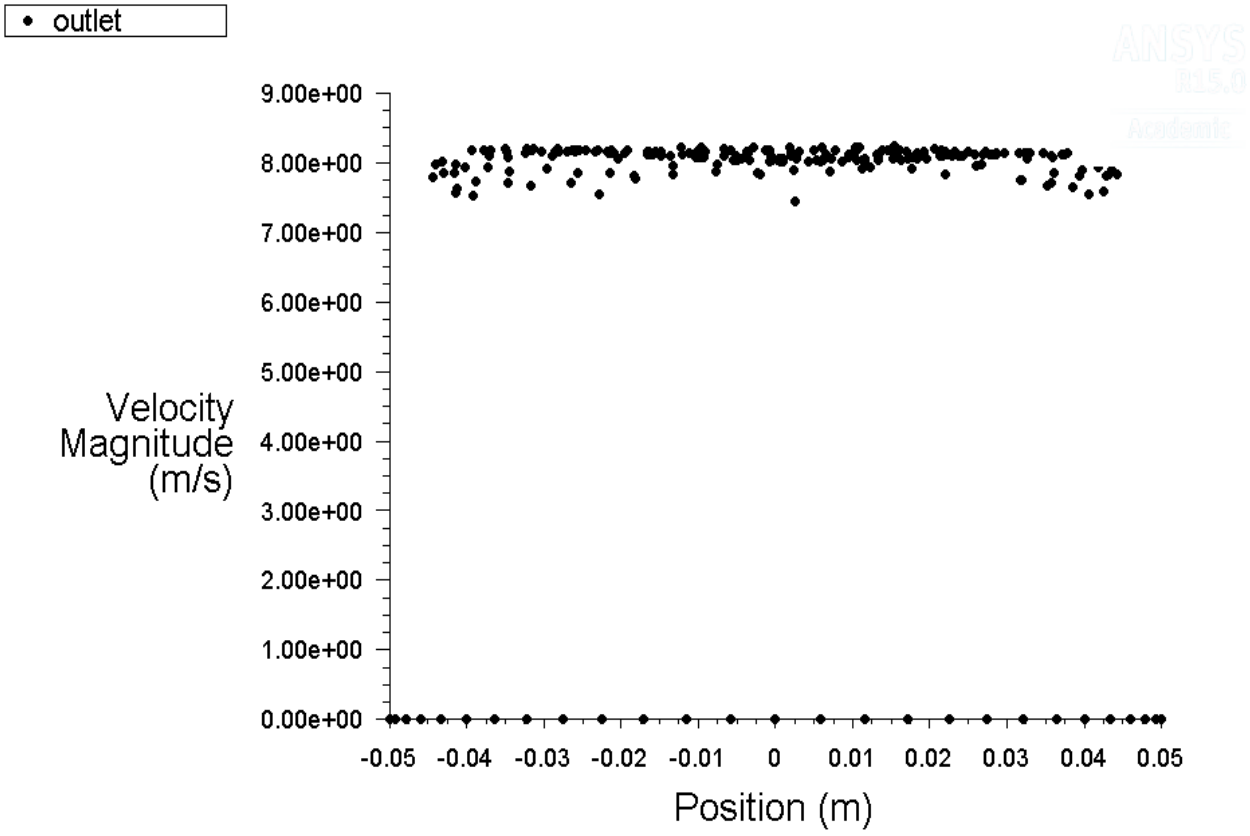

Figure 4.24: Velocity distributions at the bend outlet (r/D = 2.5) at 2 m/s

4.8 Erosion Rate Distribution at the Pipe Wall

The erosion wear caused by the impact of particles is randomly distributed at the pipe wall. Many parameters like pipe geometry, flow velocity affects the occurrence of erosion as the slurry motion gets deviated under the influence of such parameters. To observe the occurrence location of erosion wear, several distributions of erosion are plotted on the pipe bend wall having diameter in range of 50 to 250 mm at 2 and 8 m/s velocity. Figure 4.25 to 4.34 represents the erosion distribution at the pipe wall. At flow velocity of 2 m/s more erosion rate is observed form smaller diameter pipes and it is located mostly along the bend curvature while significantly less erosion was also observed near the inlet and outlet of curvature. A reduction in erosion rate is noticed as the pipe diameter increases. The distribution shows almost negligible erosion wear for higher diameter pipes at 2 m/s velocity.

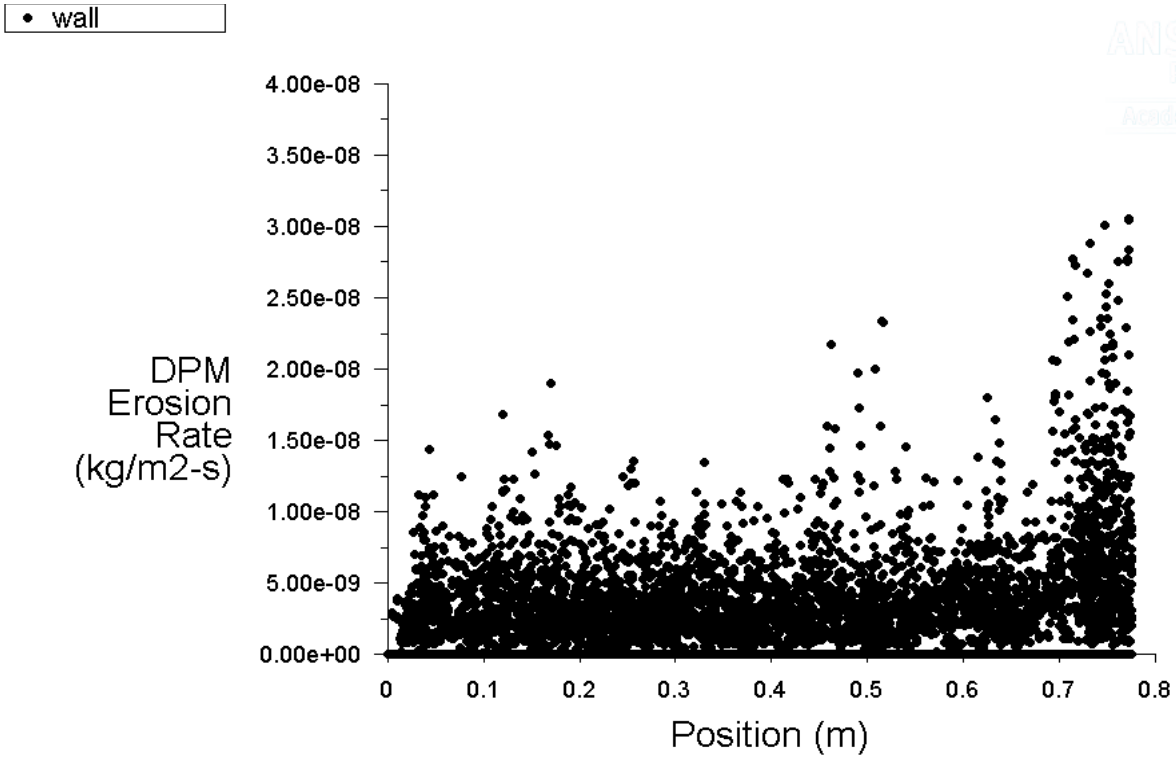

Figure 4.25: Erosion rate distributions along the wall of 50 diameter bend at 2 m/s

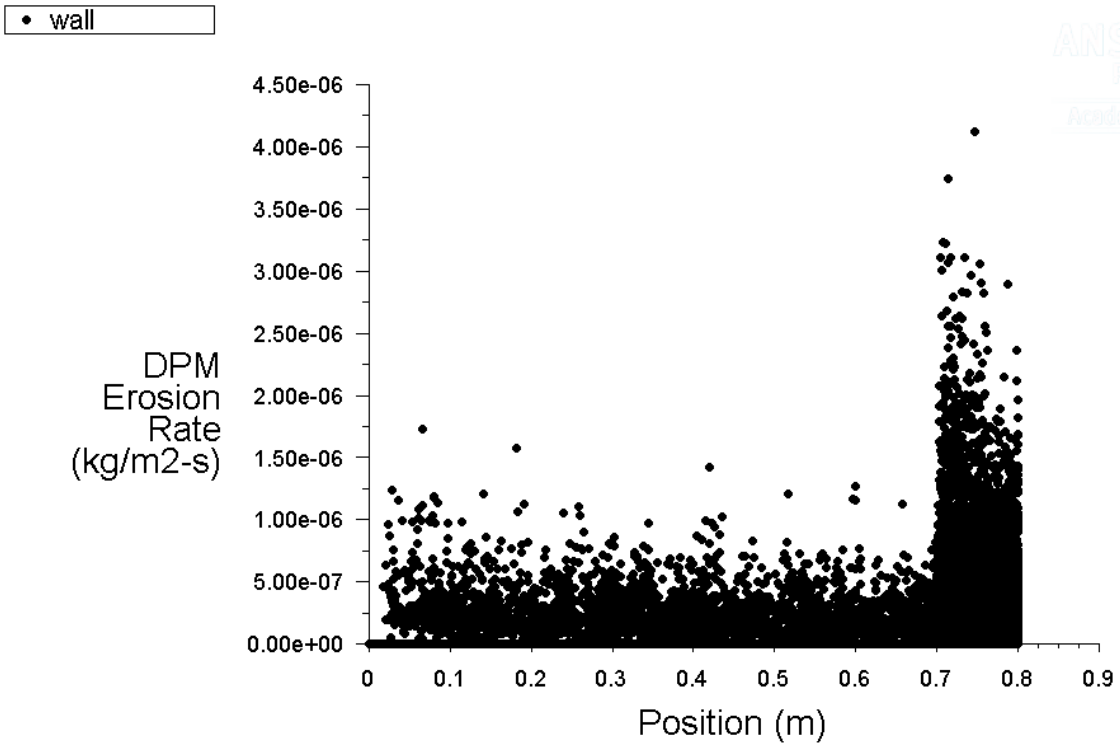

Figure 4.26: Erosion rate distributions along the wall of 100 diameter bend at 2 m/s

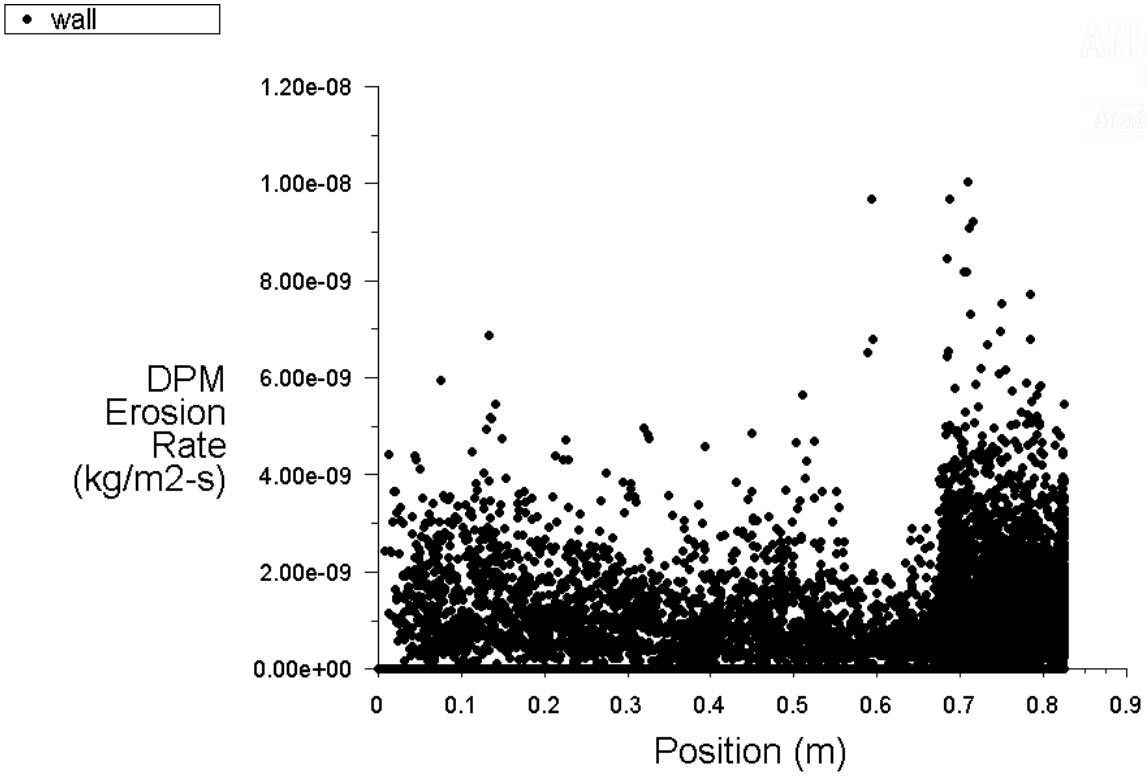

Figure 4.27: Erosion rate distributions along the wall of 150 diameter bend at 2 m/s

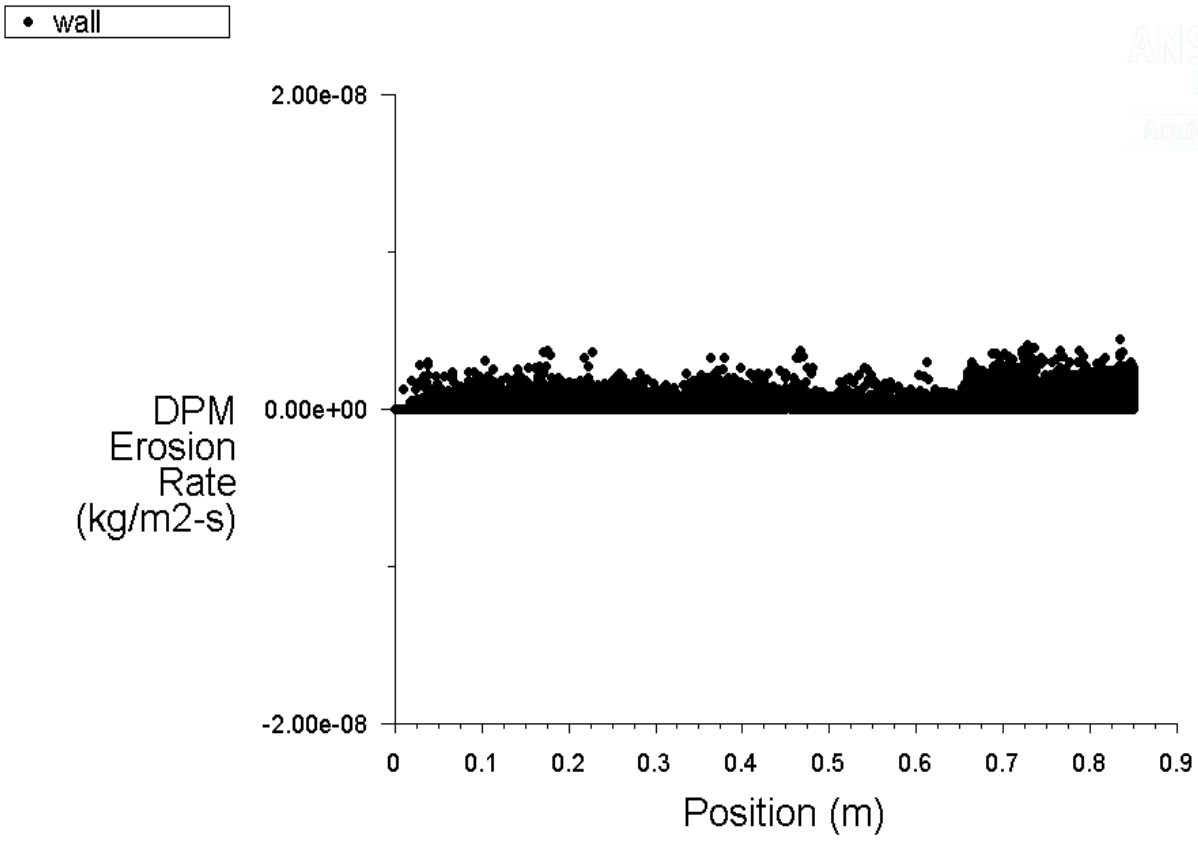

Figure 4.28: Erosion rate distributions along the wall of 200 diameter Bend at 2 m/s

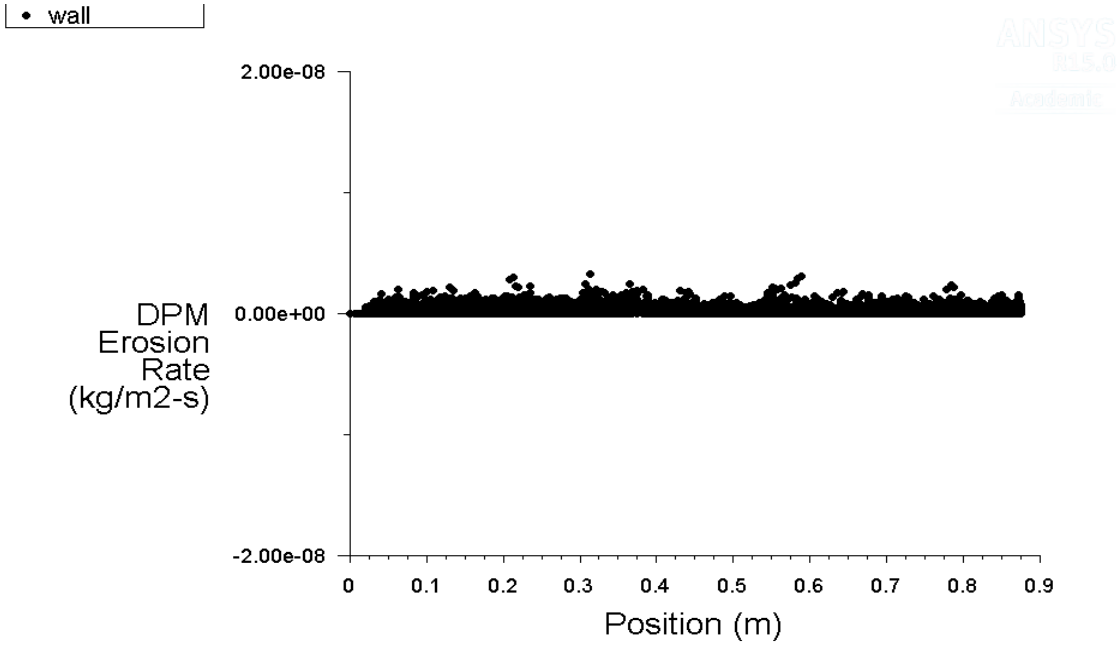

Figure 4.29: Erosion rate distributions along the wall of 250 diameter Bend at 2 m/s

When the velocity exceeds from low to high value then exponential growth in erosion rate is observed. It can be noticed that the erosion rate is much higher for the low diameter pipe. The

location of erosion rate for low diameter pipes was found near the entrance of the bend and it gains maximum magnitude near concave wall of the bend curvature while minimum erosion is observed at convex wall. For higher diameter pipes the erosion rate is significantly less than low diameter pipes at the same velocity.

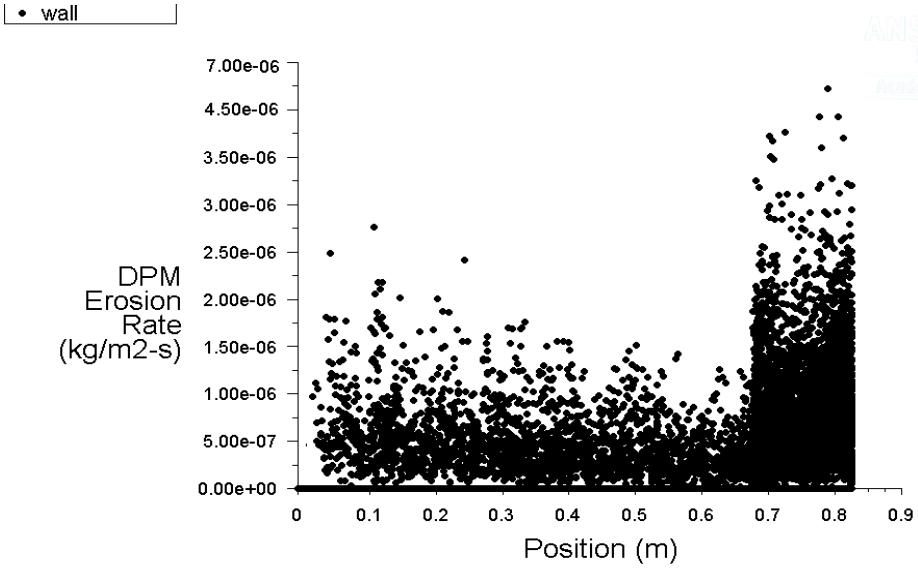

Figure 4.30: Erosion rate distributions along the wall of 50 diameter Bend at 8 m/s

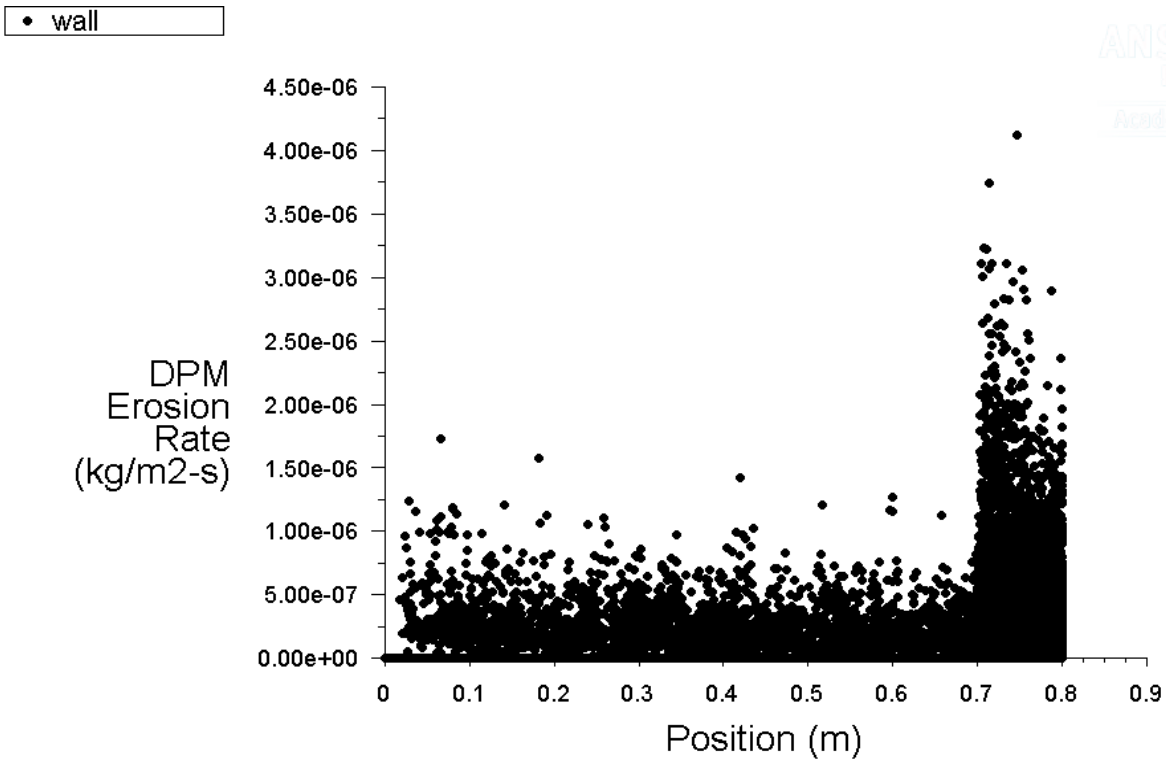

Figure 4.31: Erosion rate distributions along the wall of 100 diameter Bend at 8 m/s

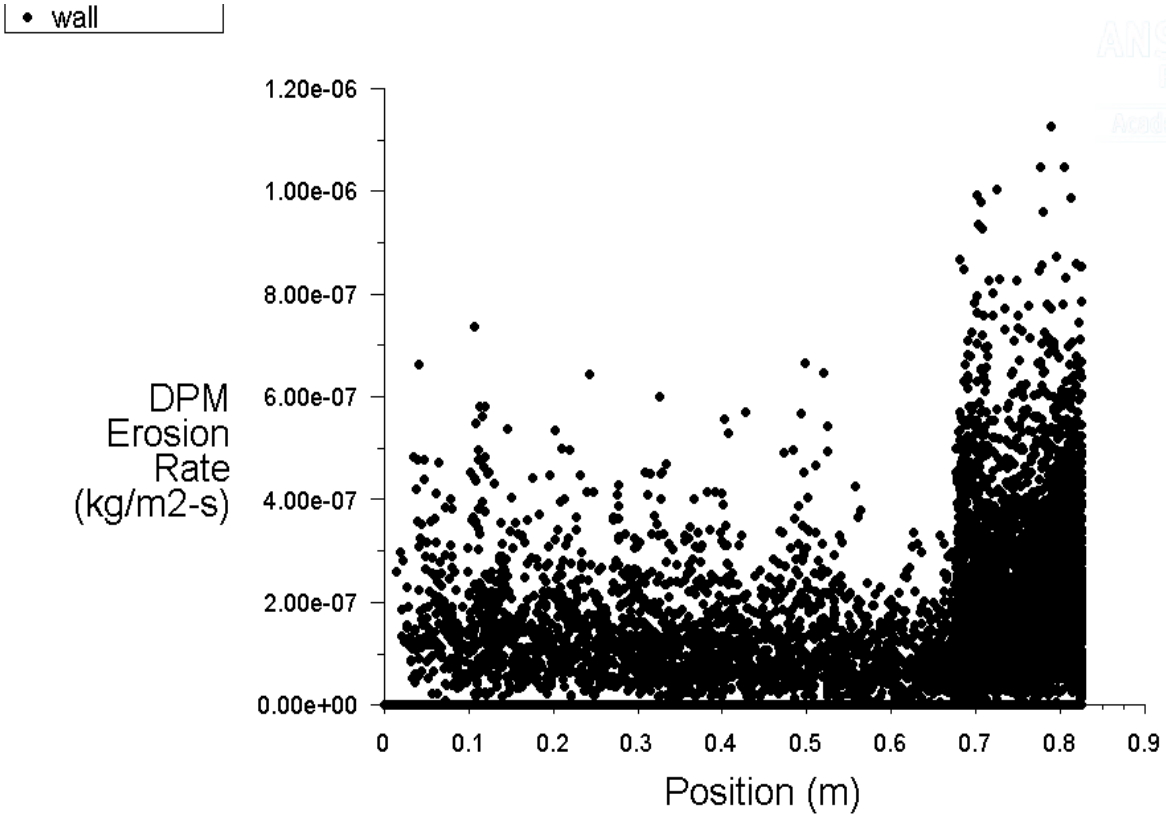

Figure 4.32: Erosion rate distributions along the wall of 150 diameter bend at 8 m/s

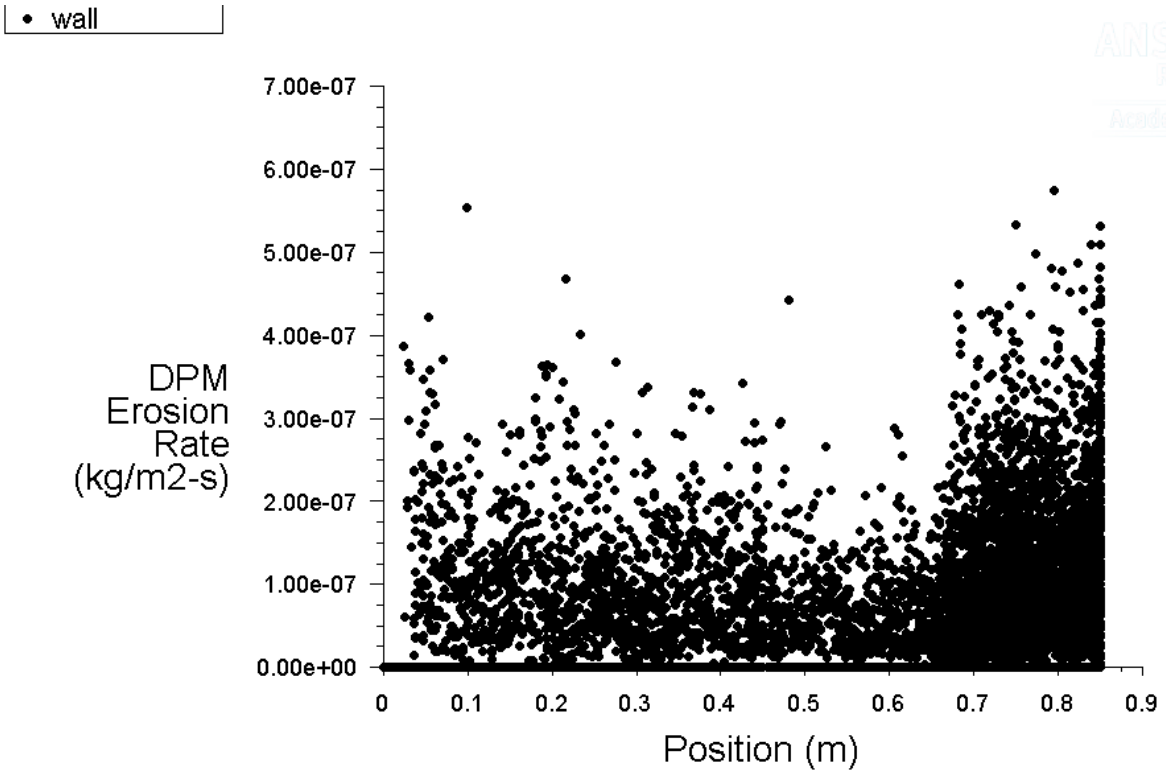

Figure 4.33: Erosion rate distributions along the wall of 200 diameter bend at 8 m/s

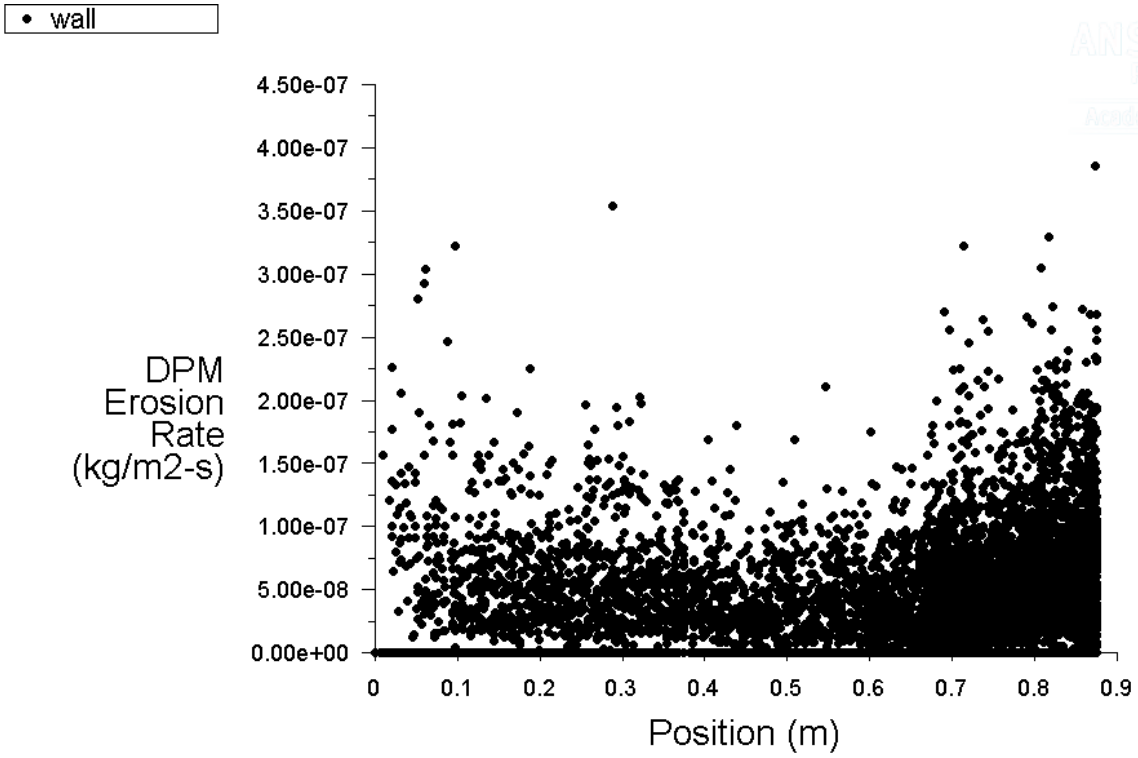

Figure 4.34: Erosion rate distributions along the wall of 250 diameter bend at 8 m/s

CHAPTER 5

CONCLUSION

In this work, investigations are carried out to evaluate the erosion wear of mild steel pipe bend for the slurry flow of bottom ash and water by using CFD code FLUENT 15.0. The Euler-Lagrange approach with standard k- ε turbulent modeling scheme is applied. Simulation study is carried by considering several pipe bends of different diameters from 50 to 200 mm, bending angles in range of 45 to 90^0 and bending radius ratio of 1.5 to 2.5 at flow velocity variation from 2 to 8 m/s. An attempt is made to evaluate the influence of bending angles, pipe diameters, flow velocity and bending radius on the erosion wear. The following important results can be concluded from the present investigation:

- By analysing the erosion wear for pipe of different bending angles, it is noticed that larger angled bend suffered with more erosion. The erosion rate for 90^0 bend is found to be 63% more than the 45^0 bend at the same velocity of 8 m/s.
- Less erosion wear is found near the entrance of pipe bend and it becomes maximum across 30-60^0 of bend curvature.
- Inverse relationship between erosion rate and pipe diameter is observed. Total 12 times reduction of maximum erosion rate is observed as the particle diameter changes from 50 mm to 250 mm. Erosion wear reduction is found to get stabilized for pipe bends having diameter of 200 mm or above on keeping other parameter fixed.
- Complete change in the magnitude of maximum erosion rate was observed when the flow velocity exceeds from low to high value. Total 13 times increment in erosion rate is noticed on 150 mm diameter 90^0 pipe bend when the velocity exceeded from 2 to 8 m/s.
- Low erosion rate is found on the large bending radius pipes. Approximately 50% reduced erosion wear is observed when the bending radius to pipe diameter ratio changes from 1.5 to 2.5. The fluid flow in larger radius bend is seems to be more similar to the flow in straight pipe.

5.1 Future Scope of the Work

The present simulation study has been performed to predict the erosion wear on different components of slurry transport pipe line like straight pipes and pipe bends with different diameter, bending angles and bending radius at different operating conditions. This study can also be continuing for erosion wear prediction caused by multiphase flow on industrial pipe lines and slurry pumps.

References

[1] O. P. Modi, R. Dasgupta, B. K. Prasad, A. K. Jha, A. H. Yegneswaran, and G. Dixit, "Erosion of a High-Carbon Steel in Coal and Bottom-Ash Slurries," *Journal of Material Engineering and Performance,* vol. 9, no. October, pp. 522–529, 2000.

[2] E. Sequoia, E. Raask, and R. April, "Tube Erosion by Ash Impaction," *Wear,* vol 13, pp 301-315, 1969.

[3] S. Behera, A. K. Sahu, S. Das, P. K. Senapati, and S. K. Mishra, "Scale-Up Design and Erosion Studies of Bottom Ash in Pneumatic Conveying System," *Coal Combustion and Gasification Products* vol. 5, pp. 1–8, 2013.

[4] D. O. Njobuenwu and M. Fairweather, "Modelling of Pipe Bend Erosion by Dilute Particle Suspensions," *Comput. Chem. Eng.*, vol. 42, pp. 235–247, 2012.

[5] H. M. Badr and M. A. Habib, "Effect of Flow Velocity and Particle Size on Erosion in a Pipe with Sudden Contraction," vol. 5, no. December, 2002.

[6] B. Bozzini, M. E. Ricotti, M. Boniardi, and C. Mele, "Evaluation of erosion – Corrosion in Multiphase Flow via CFD and Experimental Analysis," *Wear,* vol. 255, pp. 237–245, 2003.

[7] X. Chen, B. S. McLaury, and S. A. Shirazi, "Application and Experimental Calidation of a Computational Fluid Dynamics (CFD)-based Erosion Prediction Model in Elbows and Plugged tees," *Comput. Fluids*, vol. 33, no. 10, pp. 1251–1272, 2004.

[8] M. A. Habib, H. M. Badr, and M. E. Kabir, "Erosion and Penetration rates of a Pipe Protruded in a Sudden Contraction," *Computers and FLuids* vol. 37, pp. 146–160, 2008.

[9] A. Gnanavelu, N. Kapur, A. Neville, and J. F. Flores, "An Integrated Methodology for Predicting Material Wear Rates due to Erosion," *Wear*, vol. 267, no. 11, pp. 1935–1944, 2009.

[10] M. S. Patil, E. R. Deore, R. S. Jahagirdar, and S. V Patil, "Study of the Parameters Affecting Erosion Wear of Ductile Material in Solid-Liquid Mixture," *Proceedings of the World Congress on Engineering*, vol. III, 2011.

[11] M. M. Stack and S. M. Abdelrahman, "A CFD Model of Particle Concentration Effects on Erosion-Corrosion of Fe in Aqueous Conditions," *Wear,* vol. 273, no. 1, pp. 38–42, 2011.

[12] R. Okita and S. A. Shirazi, "Experimental and Computational Investigations to Evaluate the Effects of Fluid Viscosity and Particle Size on Erosion Damage," *Journal of Fluid Engineering,* vol. 134, no. June 2012, pp. 1–13, 2015.

[13] D. O. Njobuenwu and M. Fairweather, "Modelling of Pipe Bend Erosion by Dilute Particle Suspensions," *Comput. Chem. Eng.*, vol. 42, pp. 235–247, 2012.

[14] Y. Deng, Y. Liu, J. Chen, and Y. Zhang, "Numerical Simulation of the Erosion in the 90^0 Elbow," *AIP Conf. Proc.*, vol. 1547, no. 1, pp. 671–683, 2013.

[15] H. Wu, X. Liang and Z Deng, "Numerical Simulation on Typical Parts Erosion," *Thermal Science* vol. 17, no. 5, pp. 1349–1353, 2013.

[16] R. Zhang, H. Liu, and C. Zhao, "A Probability Model for Solid Particle Erosion in a Straight Pipe," *Wear*, vol. 308, no. 1–2, pp. 1–9, 2013.

[17] V. Abdolkarimi and R. Mohammadikhah, "CFD Modeling of Particulates Erosive Effect on a Commercial Scale Pipeline Bend," *ISRN Chem. Eng.*, vol. 2013, pp. 1–10, 2013.

[18] R. Macchini, M. S. A. Bradley, and T. Deng, "Influence of Particle Size, Density, Particle Concentration on Bend Erosive Wear in Pneumatic Conveyors," *Wear*, vol. 303, no. 1–2, pp. 21–29, 2013.

[19] M. R. Safaei, O. Mahian, F. Garoosi, K. Hooman, A. Karimipour, S. N. Kazi, and S. Gharehkhani, "Investigation of Micro- and Nanosized Particle Erosion in a 90^0 Pipe Bend Using a Two-Phase Discrete Phase Model," *The Scientific World Journal*, vol. 2014, 2014.

[20] A. Mansouri, H. Arabnejad, S. a Shirazi, and B. S. Mclaury, "A Combined CFD / Experimental Methodology for Erosion Prediction," *Wear*, pp. 1–8, 2014.

[21] Q. H. Mazumder, "Effect of Particle Size on Magnitude and Location of Maximum Erosion in S-Bend," *Journal of Pressure Vessel Technology*, vol. 2015, pp. 1–6, 2014.

[22] L. Zeng, G. A. Zhang, and X. P. Guo, "Erosion–Corrosion at Different Locations of X65 Carbon Steel Elbow," *Corros. Sci.*, vol. 85, no. 0, pp. 318–330, 2014.

[23] A. I. Shahata, M. T. Youssef, K. Saqr, and M. Shehadeh, "CFD Investigation of Slurry Seawater Flow Effect in Steel Elbows," *IJERT* vol. 3, no. 1, pp. 364–370, 2014.

[24] H. Hadžiahmetović, N. Hodžić, D. Kahrimanović, and E. Džaferović, "Computational Fluid Dynamics (CFD) Based Erosion Prediction Model in Elbows," *Tech. Gaz.*, vol. 3651, pp. 275–282, 2014.

[25] M. Jafari, Z. Mansoori, M. Saffar Avval, and G. Ahmadi, "The Effects of Wall Roughness on Erosion Rate in Gas–Solid Turbulent Annular Pipe Flow," *Powder Technol.*, vol. 271, pp. 248–254, 2015.

[26] C. B. Solnordal, C. Y. Wong, and J. Boulanger, "An Experimental and Numerical Analysis of Erosion Caused by Sand Pneumatically Conveyed Through A Standard Pipe Elbow," *Wear*, vol. 336–337, pp. 43–57, 2015.

[27] S. Shamshirband, A. Malvandi, A. Karimipour, M. Goodarzi, M. Afrand, D. Petković, M. Dahari, and N. Mahmoodian, "Performance Investigation of Micro- And Nano-Sized Particle Erosion In A 90° Elbow Using an ANFIS Model," *Powder Technol.*, vol. 284, pp. 336–343, 2015.

[28] A. López, W. Nicholls, M. T. Stickland, and W. M. Dempster, "CFD Study of Jet Impingement Test Erosion Using Ansys Fluent and OpenFOAM," *Comput. Phys. Commun.*, 2015.

[29] A. Khan "Effect of Slurry Concentration on Erosion Wear of Mild Steel," *International Journal in Applied Studies and Production Management*, vol. 1, no. 4,

pp. 17–21, 2015.

[30] C. A. R. Duarte, F. J. de Souza, and V. F. dos Santos, "Numerical Investigation of Mass Loading Effects on Elbow Erosion," *Powder Technol.*, vol. 283, pp. 593–606, 2015.

[31] J. Chen, Y. Wang, X. Li, R. He, S. Han, and Y. Chen, "Erosion Prediction of Liquid-Particle Two-Phase Flow in Pipeline Elbows via CFD–DEM Coupling Method," *Powder Technol.*, vol. 275, pp. 182–187, 2015.

[32] W. Peng and X. Cao, "Numerical Prediction of Solid Particle Erosion in Pipe Bends With Liquid–Solid Flow," *Powder Technol.*, vol. 294, pp. 266–279, 2016.

Communications

V. Kannojiya, S. Kumar, M. Kanwar and S.K. Mohapatra, “Simulation of erosion wear in slurry pipe line using CFD,” *Applied Mechanics and Materials.*